Short Title: Interplay between autophagy and lipid metabolism

***Corresponding author information:**

Tamar Avin-Wittenberg
Department of Plant and Environmental Sciences,
Alexander Silberman Institute of Life Sciences,
The Hebrew University of Jerusalem,
9190401, Jerusalem, Israel
E-mail: tamar.avin-wittenberg@mail.huji.ac.il
Tel: +972 2 5494023

Wagner L. Araújo
Departamento de Biologia Vegetal,
Universidade Federal de Viçosa,
36570-900 Viçosa, Minas Gerais, Brazil
E-mail: wlaraujo@ufv.br
Tel: +55 31 3612.5358

Title:

Autophagy is required for lipid homeostasis during dark-induced senescence in Arabidopsis

Authors: Jessica A. S. Barros[a,b], Sahar Magen[b], Taly Lapidot-Cohen[c], Leah Rosental[c], Yariv Brotman[c], Wagner L. Araújo[a*] and Tamar Avin-Wittenberg[b*]

Affiliation:

[a] Departamento de Biologia Vegetal, Universidade Federal de Viçosa, 36570-900 Viçosa, Minas Gerais, Brazil

[b] Department of Plant and Environmental Sciences, Alexander Silberman Institute of Life Sciences, Hebrew University of Jerusalem, Givat Ram, 9190401, Jerusalem, Israel

[c] Department of Life Sciences, Ben-Gurion University of the Negev, 8410501, Beer-Sheva, Israel

*Author for Correspondence

One-sentence summary: Autophagy is required for the mobilization of membrane lipid components and lipid droplet dynamics during extended darkness in *Arabidopsis*.

Author contributions:

J.A.S.B., W.L.A, and T.A-W.. designed the research; J.A.S.B. performed most of the research; T.A-W. and W.L.A. supervised the project; Y.B. contributed with new reagents/analytic tools for lipid analysis; S.M contributed with transcript and western blot analysis; T.L-C performed lipid profile; L.R. performed the free fatty acid analysis; J.A.S.B., W.L.A., and T.A-W. analyzed the data and wrote the article with contributions of all the authors.

Funding information:

This work was made possible through financial support from the Serrapilheira Institute (grant Serra-1812-27067). Work at the TAW group is supported by the Israeli Science Foundation, grant number 1899/16. Scholarships granted by the National Council for Scientific and Technological Development (CNPq-Brazil) and Council for Higher Education (Malag-Israel) to JASB and research fellowships awarded by CNPq-Brazil to WLA are also gratefully acknowledged.

Abstract

Autophagy is an evolutionarily conserved mechanism that mediates the degradation of cytoplasmic components in eukaryotic cells. In plants, autophagy has been extensively associated with the recycling of proteins during carbon starvation conditions. Even though lipids constitute a significant energy reserve, our understanding of the function of autophagy in the management of cell lipid reserves and components remains fragmented. To further investigate the significance of autophagy in lipid metabolism, we performed an extensive lipidomic characterization of Arabidopsis (*Arabidopsis thaliana*) autophagy mutants (*atg*) submitted to dark-induced senescence conditions. Our results revealed an altered lipid profile in *atg* mutants, suggesting that autophagy affects the homeostasis of multiple lipid components under dark-induced senescence. The acute degradation of chloroplast lipids coupled with the differential accumulation of triacylglycerols (TAGs) and plastoglobuli indicates an alternative metabolic reprogramming towards lipid storage in *atg* mutants. The imbalance of lipid metabolism compromises the production of cytosolic lipid droplets and the regulation of peroxisomal lipid oxidation pathways in *atg* mutants.

Introduction

The precise control of energy homeostasis is crucial for plant survival, particularly under biotic and abiotic stress conditions. Under low energy availability, plants require a strategy other than carbohydrate oxidation to fully sustain energy production. Therefore, proteins, lipids, and chlorophylls can be catabolized instead of sugars to provide alternative substrates for the tricarboxylic acid (TCA) cycle. This assures the continued operation of the mitochondrial electron transport chain (Ishizaki et al., 2005; Kunz et al., 2009; Araujo et al., 2011; Hortensteiner & Krautler, 2011).

Among the alternative substrates of respiration in plants, lipids comprise a significant carbon reserve that represents an important alternative source of energy. Although in comparison to carbohydrates, the usage of lipids is less efficient, as assessed by the respiratory quotient, their intracellular storage and utilization are critical for the maintenance of cellular energy homeostasis (Araujo et al., 2011; Yang et al., 2018). Plants store lipids as the neutral lipid species TAG (Yang et al., 2018). In leaf mesophyll cells, TAGs are deposited in specialized storage compartments, namely lipid droplets (LDs) in the cytosol or plastoglobuli (PG) inside chloroplasts (Van wick et al., 2017). During nutrient deprivation, cellular lipid reserves are hydrolyzed into fatty acids (FAs), which are further catabolized during β-oxidation. Accordingly, mutants with dysfunctional β-oxidation, triggered by the disruption of the PEROXISOMAL ABC TRANSPORTER 1 (PXA1), exhibit hypersensitivity to extended darkness (Kunz et al., 2009). Moreover, several transcripts of the β-oxidation pathway are up-regulated during developmental leaf senescence (Troncoso-Ponce et al., 2013).

Autophagy, one of the primary cellular catabolic process, is involved in the degradation and recycling of cytoplasmic constituents into primary metabolites (Avin-Wittenberg et al., 2018). The autophagy mechanism is governed by autophagy-related (*ATG*) genes that are highly conserved among eukaryotes (Marshall and Vierstra, 2018). Plants with genetic disruption of *ATG* genes (hereafter *atg* mutants) have been well characterized for sensitivity to several stresses, particularly nutrient starvation (Avin-Wittenberg, 2018). The importance of autophagy in plants has been mostly associated with the recycling of proteins to amino acids under starvation conditions (Izumi et al., 2013; Li et al., 2014, Barros et al., 2017: Hirota et al., 2018; Mcloughin et al., 2018, 2020). By contrast, in mammals and yeast, autophagy has been largely associated not only with proteins but also with lipid metabolism (Elander et al., 2018; Barros et al., 2020). Accordingly, it was shown that autophagy supplies FAs for LD biogenesis as

well as mediates the selective degradation of LDs in both mammals and yeast (Singh et al., 2009; Rambolt et al., 2015; Ngyugen et al., 2017).

A growing body of evidence suggests a dual role of autophagy in the lipid metabolism of alga and plants. Thus, in Chlamydomonas (*Chlamydomonas reinhardtii*), it has been postulated that autophagy participates in both TAG biosynthesis and LD formation (Couso et al., 2017; Pugkaew et al., 2017). In addition, microscopic evidence pointed to the autophagy-mediated engulfment of LDs in the algae *Auxenochlorella protothecoides* (Zhao et al., 2014) and *Micrasterias denticulata* (Schwarz et al., 2017). Interestingly, recent data also suggested that autophagy may mediate LD formation during an early stage of starvation while likely operating in LD degradation at the later stages of nitrogen starvation in Chlamydomonas (Tran et al., 2019).

In vascular plants, it was demonstrated that autophagy contributes to TAG synthesis via the turnover of organellar membranes in Arabidopsis under normal growth conditions (Fan et al., 2019). On the other hand, it was suggested the autophagy operates in the degradation of LDs by a selective microautophagy mechanism under extended darkness (Fan et al., 2019). Notably, this study was based on the analysis of Aradiposis mutants overexpressing the LD marker OLE1-GFP and knockout for SUGAR DEPENDENT-1 (SDP1) lipase, which are genotypes with altered LD and TAG metabolism (Fan et al., 2013, 2017; Barros et al., 2020). In maize (*Zea mays*), *atg12-1* mutant presented a higher LD number, which could reflect active LD assembly or disruption of LD catabolism (Mcloughin et al., 2020). It remains contentious, however, whether autophagy mediates the biogenesis or degradation of LDs in vegetative tissues (Elander et al., 2018; Barros et al., 2020; Masclaux-Daubresse et al., 2020). Although recent studies have clearly revealed an interplay between autophagy and lipid metabolism (Mcloughin et al.,2018, 2020; Have et al., 2019; Fan et al., 2019), relatively little is known about the role of autophagy in the mobilization of lipid components under energy limitation conditions.

Here, we investigated the significance of autophagy in lipid metabolism during dark-induced senescence in Arabidopsis. By performing an extensive lipidomic analysis of three independent *atg* mutants, we observed an overall impact of autophagy deficiency on all lipid classes analyzed and the free fatty acid (FFA) profile. The differential pattern of phospholipid levels and TAG accumulation was further coordinated with changes in LD number and PG size. In addition, analysis of β-oxidation genes revealed an induction of lipid oxidation pathways in *atg* mutants.

168 Collectively, our results demonstrate that autophagy is an essential component in the
169 management of lipid reserves, affecting membrane lipid mobilization, the balance of LD
170 and PG formation, and the regulation of β-oxidation pathways under dark-induced
171 senescence.
172
173

Results

Differential lipid response of *atg* mutants under dark-induced senescence

To examine the involvement of autophagy in lipid remodeling during dark-induced senescence, we analyzed three previously described Arabidopsis autophagy mutants: *atg5-1* and *atg7-2* with full inhibition of autophagy (Chung et al., 2010); and *atg9-4* mutant that displayed a milder reduction of the autophagic process (Shin et al., 2014). The experimental setup consisted of the submission of 4-week-old plants to extended darkness conditions, a system widely used to induce energetic stress in plants (Ishizaki et al., 2005; Araujo et al., 2010; Barros et al., 2017).

To further investigate the impact of autophagy disruption on lipid homeostasis during dark-induced senescence, we performed Liquid Chromatography–Mass Spectrometry lipidomic analysis of *atg5-1*, *atg7-2*, *atg9-4,* and their corresponding wild-type (WT) plants. We were able to identify 119 lipid species of the following classes: Phosphatidylcholine (PC), Phosphatidylethanolamine (PE), Diacylglycerol (DAG), Triacylglycerol (TAG), Monogalactosyldiacylglycerol (MGDG), and Digalactosyldiacylglycerol (DGDG). We first performed a principal component analysis (PCA) based on the lipid profiles of samples from control and 6 days (d) of darkness (Fig. 1). Most of the variance of the dataset was covered by the first two principal components, explaining 69.1% of the overall data variance (57.8% and 11.3% for PC1 and PC2, respectively). This fingerprint analysis allowed us to obtain a general picture, discerning the main differences between the darkness treatment and the *atg* mutant lines. Briefly, it revealed that under control conditions (before darkness treatment), all genotypes clustered together; however, a clear separation according to the treatment and genotype was observed following darkness, wherein *atg7-2* and *atg5-1* were disconnected of the WT samples (Fig. 1). Interestingly, *atg9-4* presented an intermediary distribution, sharing certain metabolic similarities with WT and the other *atg* genotypes. The analysis of all data points also highlighted the delayed response of *atg9-4,* which after 6d and 9d of darkness, was more closely related to *atg5-1* and *atg7-2* after 3d of darkness conditions (Supplemental Figure S1).

Our results are in close agreement with the milder impact of the *ATG9* disruption on metabolic features previously reported under dark-induced senescence (Barros et al., 2017). This response was related to residual autophagy activity observed in *atg9* lines (Yoshimoto et al., 2004; Shin et al., 2014), which explains the intermediary lipid response of *atg9-4* genotype. The information of the individual variables that

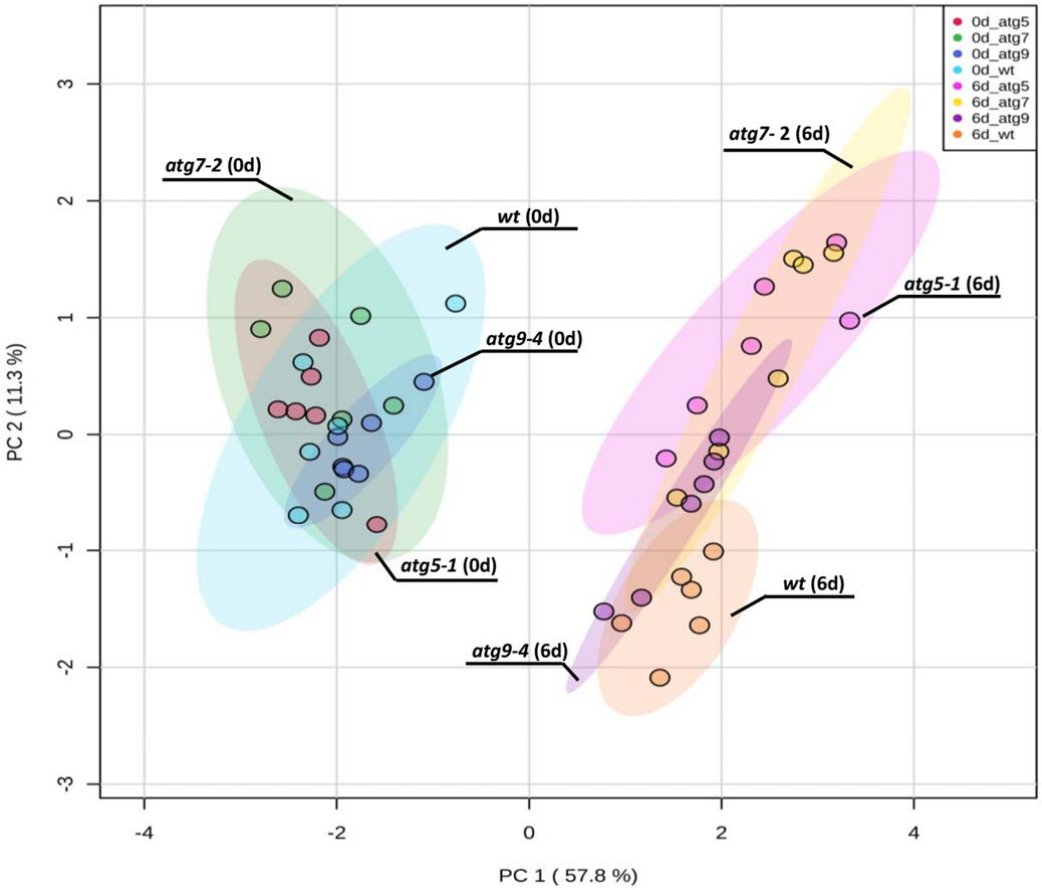

Figure 1 - Differential lipid response of *atg* mutants under dark-induced senescence. Principal component analysis (PCA) was performed using the lipid data obtained in samples from 4-week-old Arabidopsis plants immediately before lights were turned off (0 d) and after further treatment for 6d in darkness. Three loss-of-function mutants of the autophagy pathway, namely *atg5-1, atg7-2, atg9-4* and their respective wild type (WT) were analyzed.

contributed most to PC1 and PC2 (i.e., the lipids with the main impact on the variance of the dataset) is additionally available in Supplemental Table S1. Several lipids accounted for the main changes observed in the PCA. Briefly, PC1 was mainly comprised of MGDG 34:4, MGDG 34:3, PC 38:4(1) and MGDG 34:1 underlining the separation of darkened and control samples. On the other hand, TAG 54:9, MGDG 32:3 (1), and TAG 52:6 were the main lipids responsible for changes in PC2 (Supplemental Table 1), contributing to the differences between the genotypes under darkness (Fig. 1).

The lack of autophagy affects the dynamics of phospholipids during dark-induced senescence

In order to obtain a more detailed characterization of the lipid composition of *atg* mutants following extended darkness, we analyzed each lipid class separately. We

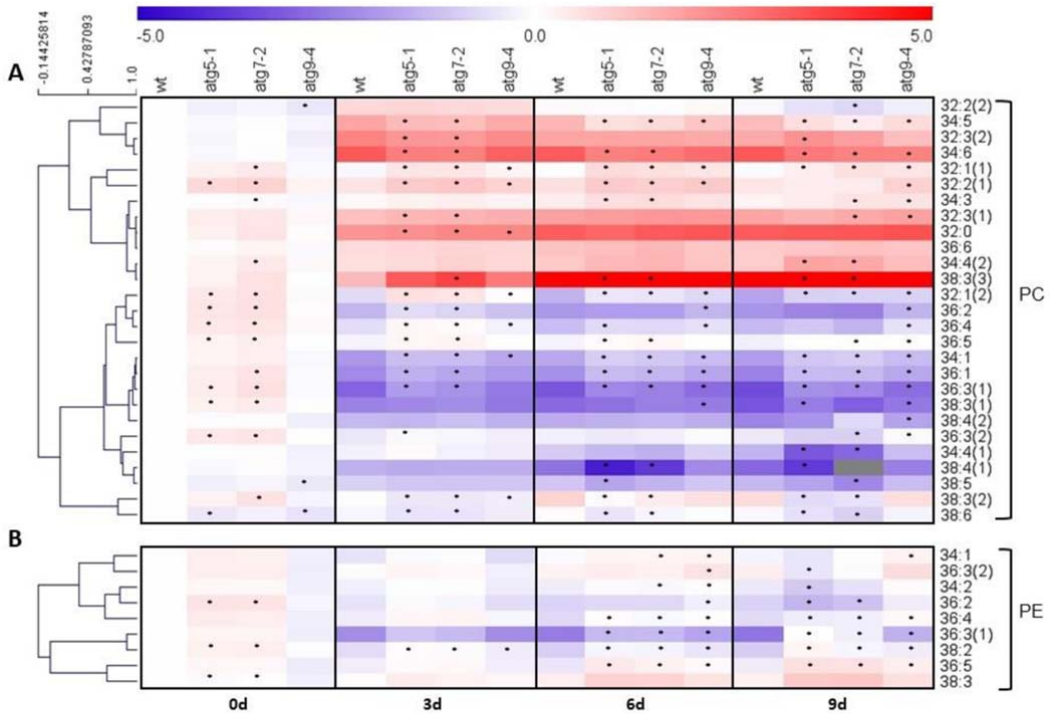

Figure 2 - *atg* mutants present altered phospholipid levels under control and extended darkness conditions
Hierarchical clustering of (A) Phosphatidylcholine (PC) and (B) Phosphatidylethanolamine (PE). Values plotted are $\log_2$ fold change. Distances were measured by Pearson correlation using MeV 4.9.0 software. Data were normalized to the mean response calculated for the 0-d dark treated leaves of the wild type (WT). Values presented are means ± SE of five-six biological replicates per genotype; an asterisk (*) designates values that were determined by Student's t-test to be significantly different ($P < 0.05$) from WT at each time point analyzed.

220 were able to identify the two dominant structural phospholipid species, namely PC and
221 PE. These lipids are components of the plasma membrane, in which PC is associated
222 with the outer leaflet, and PE is concentrated in the inner leaflet. PC and PE are also
223 precursors of lipid mediators, such as phosphatidic acid (PA) and diacylglycerol (DAG)
224 (Wang et al., 2006; Testerink and Munnik, 2011). Additionally, PE plays a crucial role
225 in autophagosome formation (Soto-Burgo et al., 2018; Barros et al., 2020).
226 Interestingly, a slight accumulation of both PC and PE was observed in *atg5-1* and *atg7-*
227 *2* mutants before darkness treatment (control conditions, Fig. 2 – 0d). The difference of
228 PC levels under control conditions was marked by the accumulation of 36C PC in *atg5-*
229 *1* and *atg7-2* mutants, whereas no significant changes were observed in *atg9-4* at this
230 time point (Fig. 2A – 0d). Extended darkness triggered a mixed response of different PC
231 species. Thus, the levels of 32C and 34C mostly increased in WT plants under darkness.
232 However, *atg5-1* and *atg7-2* presented lower accumulation of 34C PC species that
233 contain a combination of 18C and 16C polyunsaturated acyl species, such as 34:5-
234 (18:3-16:2-) and 34:6- (18:3-16:3) during dark treatment. The PC containing FAs with
235 longer chains, 36C and 38C, were generally reduced in response to extended darkness.

However, *atg5-1* and *atg7-2* presented a milder reduction of 36C PC species after 3d and 6d of darkness, whereas the 38C species (38:3(2), 38:4, 38:5, 38:6) were more reduced in these genotypes after 6d and 9d of darkness (Fig 2A).

Following dark treatment, the majority of PE species decreased in WT plants; however, this reduction was milder in *atg* mutant lines after 6d of darkness (Fig. 2B). On the other hand, after 9d of darkness, species such as PE 36:2, 34:2, and 36:3(2) were highly reduced in *atg5-1* and *atg7-2* compared to WT. Surprisingly, the PE species 36:5 and 38:3 presented a contrasting pattern, accumulating after 6d and 9d of darkness in *atg* mutants (Fig. 2B).

Impairment of autophagy accelerates the loss of chloroplast lipids

Since chloroplast lipids are subjected to constant turnover during senescence, we next evaluated the predominant lipid constituents of chloroplast membranes, MGDG and DGDG. An apparent reduction in more than 90% of the detected MGDGs and DGDGs was observed in *atg* mutants exposed to dark treatment (Fig. 3). This response was intensified throughout the dark treatment, and thus the levels of some species were below the detection threshold after 9d. Although *atg9-4* mutants followed the same pattern, the levels of MGDG and DGDG were less reduced in comparison to *atg5-1* and *atg7-2* mutants (Fig. 3). The overall reduction of chloroplast lipids reported here is consistent with the more severe phenotype described previously for *atg5-1* and *atg7-2* mutants lines under extended darkness (Barros et al., 2017). Interestingly, slightly lower levels of unsaturated MGDG and DGDG were also observed in *atg* mutants under control conditions, highlighting the potential role of autophagy in basal chloroplast maintenance, as recently verified in different studies using both Arabidopsis *atg5* and maize *atg12* mutants (McLoughlin et al., 2018, 2020; Have et al., 2019).

Disruption of autophagy compromises TAG and LD response under dark-induced senescence

The analysis of neutral lipids revealed a general increase in TAG levels during extended darkness. TAGs are composed of three FAs esterified to a glycerol backbone (Yang et al., 2018). The dominating accumulated TAG species during dark-induced senescence harbor three FA molecule with 18C with two or three double bonds (54:7 to 54:9 in Fig. 4A), or two FA molecules with 18C with two to three double bonds and 16:3 or 16:0 as a third FA (52:5 to 52:9 in Fig. 4A). Unsaturated C18 FAs (oleic acid,

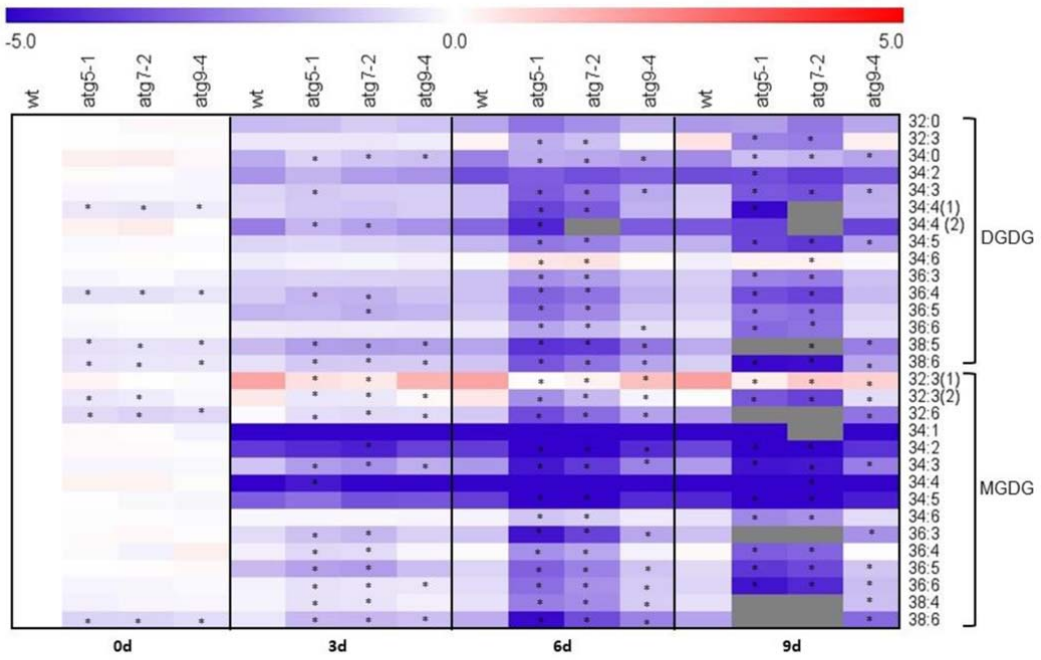

Figure 3 - Chloroplast lipids are substantially reduced in *atg* mutants during dark-induced senescence
Monogalactosyldiacylglycerol (MGDG) and Digalactosyldiacylglycerol (DGDG) values plotted are $\log_2$ fold change. Data were normalized to the mean response calculated for the 0-d dark treated leaves of the wild type (WT). Values presented are means ± SE of five-six biological replicates per genotype; an asterisk (*) designate values that were determined by the Student's t-test to be significantly different ($P < 0.05$) from WT at each time point analyzed.

18:1; linoleic acid, 18:2, and α-linolenic acid, 18:3), palmitic acid (16:0) and unsaturated C16 FAs (16:1 and 16:3) are highly abundant in chloroplasts of Arabidopsis (Hölzl and Dörmann, 2019). Our data indicate that the accumulated TAG species are most likely derived from plastidial lipids. Interestingly, the increase in chloroplast-derived TAG species was less pronounced in both *atg5-1* and *atg7-2* mutants after 3d and 6d of darkness. Additionally, an increase of other TAG species was observed from 6d of dark treatment onwards in *atg5-1* and *atg7-2* mutants, resulting in general TAG accumulation during the late period of darkness (Fig. 4A).

DAG is a central metabolite in plant lipid metabolism, serving as an intermediate of both TAG and galactolipids (Muthan et al., 2013). Similar to the observed for TAGs, the four DAG molecules identified (34:3, 34:6, 36:5, 36:6) were composed of unsaturated FAs, containing at least one unit of 16:2, 16:3 or 18:3 plastid-derived FA (Fig. 4B). Although no significant differences were observed during the early stages of dark treatment, DAGs started to accumulate 6d after the onset of dark treatment in *atg5-1* and *atg7-2* mutants. At the same time, WT and *atg9-4* plants showed a trend of reduction (Fig. 4B). The accumulation of unsaturated DAG species is likely a result of the degradation of chloroplast membranes in *atg* mutants serving as a

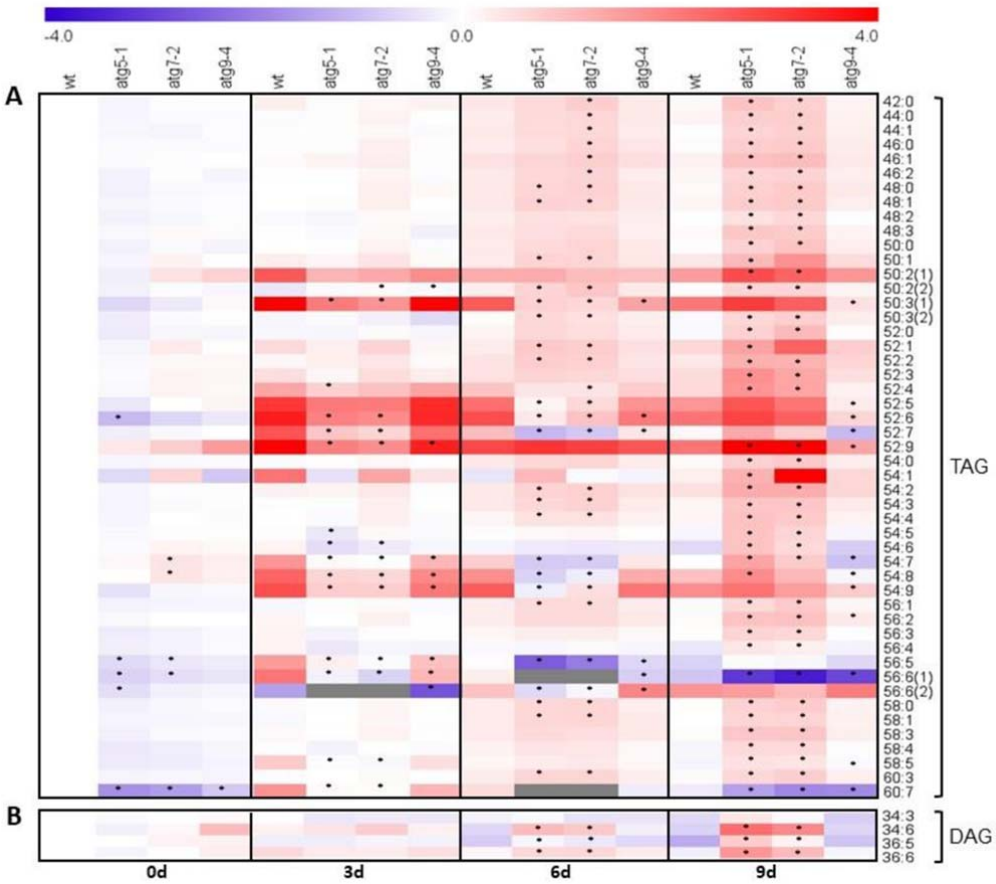

Figure 4 - Distinct accumulation of neutral lipids in *atg* mutants during dark-induced senescence
(A) Triacylglycerol (TAG) and (B) Diacylglycerol (DAG). Values plotted are $\log_2$ fold change. Data were normalized to the mean response calculated for the 0-d dark treated leaves of the wild type (WT). Values presented are means ± SE of five-six biological replicates per genotype; an asterisk (*) designates values that were determined by Student's t-test to be significantly different ($P < 0.05$) from WT each time point analyzed.

287 precursor for the general TAG accumulation in the late stages of dark-induced
288 senescence.

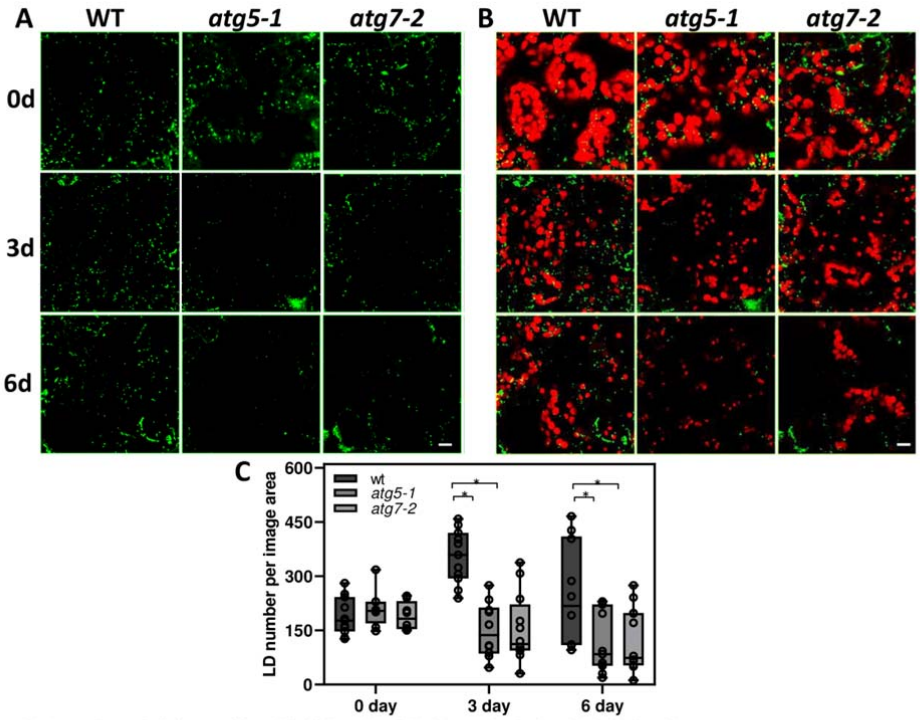

Figure 5 - Autophagy deficiency affects Lipid Droplet (LD) dynamics during dark-induced senescence
(A) Representative confocal images of LDs (BODIPY 493/503 fluorescence, false color (green) in wild type (WT), *atg5-1*, and *atg7-2* leaves. (B) Merged image of BODIPY and chloroplast autofluorescence (false color red). Images were collected at the same magnification and are projections of Z-stacks of 20 optical sections Bar = 10 µm (C) Number of total LDs per image area. The number of LDs was quantified by ImageJ as BODIPY-stained lipid area in 2D projections of Z-stacks of 3 images of four biological replicates per genotype and time point.

TAG is the central lipid reserve of the plant cell, stored in LDs (Pyc et al., 2017). To further investigate how the altered levels of TAGs in *atg7-2* and *atg5-1* mutants affect LD metabolism during dark-induced senescence, we visualized the abundance of LDs in leaf tissues by staining with the neutral-lipid-selective fluorescent dye, BODIPY493/503. An increased number of LDs was observed after 3d of darkness in WT plants (Fig. 5). However, no accumulation of LDs was observed in *atg5-1* and *atg7-2* mutants (Fig. 5). Notably, the multiple z-stacked confocal images revealed that LDs are mostly accumulated in the cytosol and not inside chloroplasts (Fig. 5A). The dynamics of LD accumulation corroborates the high levels of the plastid-derived TAG species, which were subsequently reduced after 6d of darkness in WT. Furthermore, *atg5-1* and *atg7-2* mutants displayed reduced levels of plastid-derived TAG species that can also be associated with the impairment of LD accumulation (Fig. 4A).

The disruption of autophagy triggers activation of PG metabolism

PG are specialized globular LDs composed by a membrane lipid monolayer surrounding a core of neutral lipids present in the chloroplast membranes (Van Wijck an Kessler, 2017). The production of PG is related to the accumulation of products from

306 chlorophyll and chloroplast lipid catabolism such as fatty acid phytyl esters (FAPEs),
307 TAGs and FAs (Gaude et al., 2007; Lippold et al., 2012). Given that *atg* mutants
308 presented a substantial reduction of chloroplast lipids under extended darkness, which
309 was not translated to an increase in TAGs or LD accumulation, we next investigated
310 PG-related pathways by quantitative reverse transcription (RT)-PCR. The genes phytyl
311 ester synthase 1 (*PES-1*) and *PES-2,* belonging to the esterase/lipase/thioesterase family,
312 are required for FAPE production in Arabidopsis PG during senescence (Lippold et al.,
313 2012). Accordingly, we observed an increase of *PES-1* and *PES-2* transcript levels
314 following dark-induced senescence (Fig. 6A-B). However, higher induction of *PES-1* in
315 *atg5-1* and *atg7-2*, as well as of *PES-2* in *atg7-2* mutant, was observed after 3d and 6d

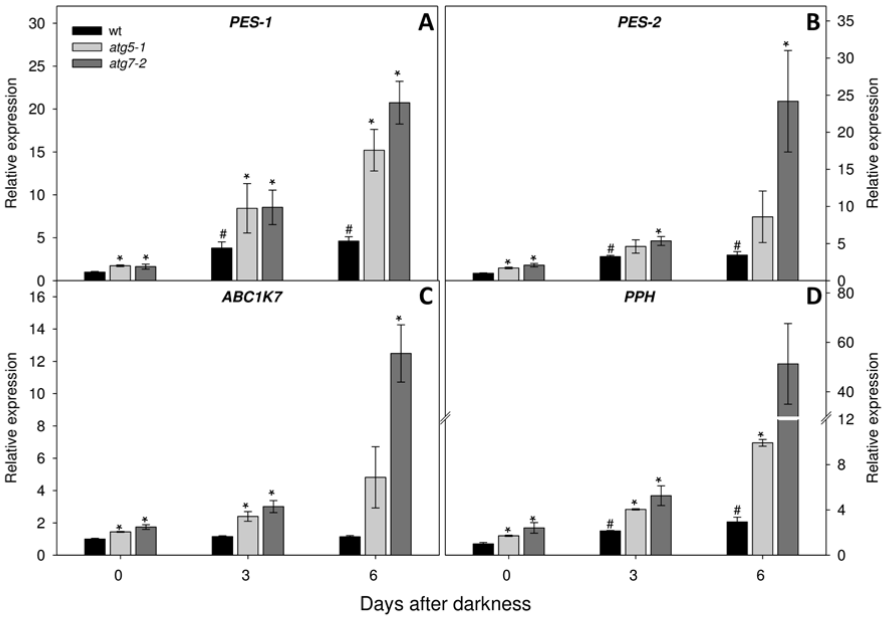

Figure 6 - PG related genes are up-regulated in *atg* mutants during dark-induced senescence
Transcript abundance is shown for genes associated with plastoglobuli (PG), including PES-1 (A), PES-2 (B), ABC1K7 (C), PPH (D). The y-axis values represent the gene expression level relative to the wild type (WT). Data were normalized with respect to the mean response calculated for the 0-d dark-treated leaves of the WT. Values presented are means ± SE of three independent biological replicates. An asterisk (*) indicates values that were determined by Student's t-test to be significantly different ($P < 0.05$) from the WT at each time point analyzed. A number sign (#) indicates values determined by Student's t-test to be significantly different ($P < 0.05$) from WT at 0d.

316 of darkness (Fig. 6A-B). The production of FAPE relies on both FFA released from
317 chloroplast membranes and phytol from chlorophyll (Lippold et al., 2012). We,
318 therefore, analyzed the chlorophyll degradation enzyme, pheophytin pheophorbide
319 hydrolase (*PPH*). As observed for *PES1* and *PES2*, the *PPH* transcript accumulated at
320 higher levels in *atg* mutants under dark-induced senescence in comparison to WT levels
321 (Fig. 6D).

322 PG serve not only as a lipid deposit but also contain an actively associated
323 proteome (Lundquist et al., 2012). The presence of several Absence of Bc1 Complex

Kinase (ABC1K) proteins was described in PG, suggesting a central role of these proteins in the regulation of PG metabolism (Ytterberg et al., 2006; Brehelin et al., 2007). The protein ABC1K7 has been characterized as a PG core component with marked accumulation during late senescence events (Lundquist et al., 2012; Bhuiyan et al., 2016). Despite the unchanged transcript levels of *ABC1K7* in WT, this gene was induced in *atg5-1* and *atg7-2* mutants following extended darkness (Fig. 6C). Although our results demonstrate a boost of PG pathways in the absence of autophagy under dark-induced senescence, *atg* mutants presented a slight but significant up-regulation for all PG-related genes even under control conditions (Fig. 6), highlighting intrinsic crosstalk between these processes.

Transmission electron microscopy analysis revealed that the number and size of PG as well as the chloroplast structure are similar in leaves of WT and *atg5-1* plants under control conditions (Figure 7A). After dark treatment, different chloroplast responses were observed in WT and *atg5-1* plants (Figure 7A). While WT presented a typical thylakoid stacking response of darkened chloroplast (Wood et al., 2019), *atg5-1* displayed smaller chloroplasts with disrupted structural remodeling, containing structures resembling senescence-associated vacuoles (Otegui et al., 2005). Moreover, a marked presence of PG was observed in *atg5-1* chloroplasts (Figure 7A). This response was ascribed to an increase in the size of PG, which reached up to 0.02 μm^2 of area (Figure 7B-C). Otherwise, WT plants also presented increases in PG size, however, to a far less extent compared to *atg5-1* mutant (Figure 7B-C).

Proteomic studies of PG have shown that members of the Fibrillin (FBN) family are the most abundant proteins in the PG proteome (Lundquist et al., 2012). Therefore, we next checked the content of the PG core protein FBN1a (Fibrillin 1a), previously characterized as a PG structural component (Austin 2006, Simkin et al., 2007, Singh et al., 2011). Immunoblotting analysis showed a strong reduction of FBN1a abudance in *atg5-1* mutant compared to WT, which display a slight increase of FBN1a abundance after 6d of dark treatment (Figure 7D and Supplemental Figure S2). Interestingly, the overexpression of FBN1a homologs resulted in increased numbers and clustering of PGs in tobacco leaves and tomato fruit (Rey et al., 2000; Simkin et al., 2007). Additionally, FBN overexpression was also associated with the delay of thylakoid disintegration, suggesting its role on protection/maintenance of chloroplast membranes (Simkin et al., 2007; Rottet al., 2015). The reduction of FBN1a protein abundance is most likely related to the occurrence of supersized PG coupled with the overall

358 degradation of chloroplast membranes in *atg5-1* mutant plants under dark-induced
359 senescence. Collectively, our findings highlight PG as a potential lipid storage site in
360 *atg* mutants submitted to extended darkness conditions. It will therefore be interesting to
361 determine hereafter whether and which extent FBNs determine PG structural modeling
362 during low energy conditions.
363
364 ***atg* Mutants induce lipid oxidation pathways in response to dark-induced**
365 **senescence**

FA oxidation may be of particular significance when the carbon and energy status is rather low. During carbon starvation, the importance of lipid metabolism was demonstrated by the characterization of β-oxidation loss-of-function mutants (Kunz et al., 2009). In addition, autophagy association with peroxisomal protein abundance was recently demonstrated (McLoughlin et al., 2018, 2020; Have et al., 2019). The general reduction of chloroplast lipids, together with reduced LD numbers in *atg5-1* and *atg7-2* mutants subjected to extended darkness, raised the question of whether these lipids were being quickly oxidized to be used as energetic substrates in *atg* mutants. We, therefore, evaluated the expression of genes related to LD catabolism and peroxisomal pathways of FA oxidation. We observed that the transcript levels of the peroxisomal enzymes

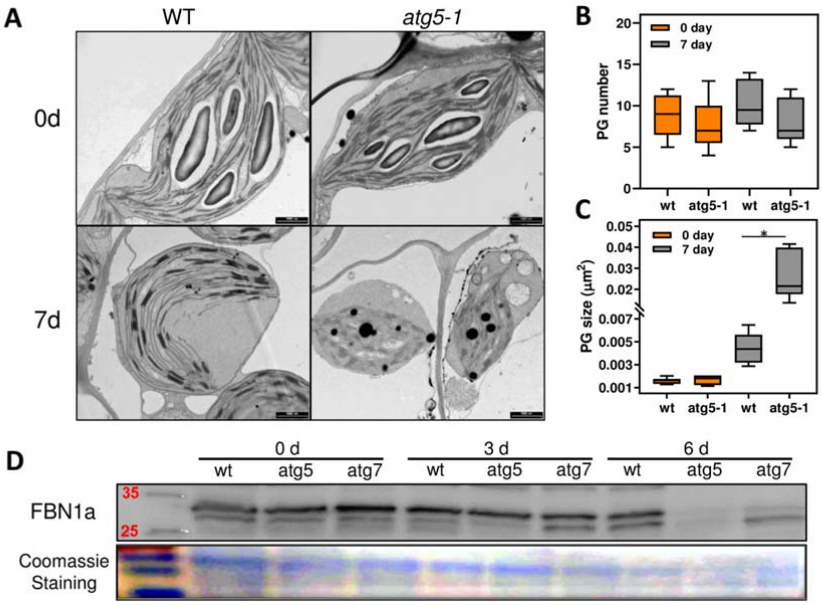

Figure 7: Autophagy disruption triggers altered PG response
(A) Transmission electron micrographs of leaves from 4-week-old Arabidopsis plants immediately before lights were turned off (0 d) and after further treatment for 7 days of darkness. Scale bar = 1 μm; Quantification of the number (B) and size (C) of plastoglobuli per chloroplasts (±SE, n= 6-7 chloroplasts of three independent cells); Analysis shown in A-C were performed in *atg5-1* and its respective wild type (WT). (D) Immunoblot analysis of the PG protein, FBN1a, was performed in leaves from 4-week-old Arabidopsis *atg5-1, atg7-2* and WT plants immediately before (0 d) and after further treatment for 3d and 6d in darkness. FBN1a protein display a predicted molecular mass to ~30-35 kD. The detection of a second lower band in the region of 30kD possibly corresponds to FBN1b protein (with high sequence similarity with FBN1a) as previously observed in Giacomelli et al., 2006; Matinis et al., 2013; 2014.

Acyl-CoA oxidase (*ACX-4*), Multifunctional protein 2 (*MPF-2*), Ketoacyl-CoA thiolase (*KAT-2*), Citrate synthase 1 (*CSY*-1) and peroxisomal Malate Dehydrogenase (*pMDH1*) genes were generally higher in *atg5-1* and *atg7-2* under extended darkness (Fig. 8 A-E). More specifically, *ACX-4* and *CSY-1* were slightly induced in WT throughout the treatment. However, higher transcript levels were observed in *atg5-1* and *atg7-2* plants

after 6d of darkness (Fig. 8A-B). Despite no major changes in *MPF-2* and *KAT-2* transcript abundance in WT plants, trends of increase were observed in *atg5-1* and *atg7-2* after 9d of darkness (Fig. 8C-D). We further confirmed that *pMDH-1* was downregulated following dark-induced senescence. *pMDH-1* operates in the reduction of oxaloacetate to malate and enables the re-oxidation of NADH for continued β-oxidation (Pracharoenwattana et al., 2007). Given that *pMDH-1* is not participating directly in β-oxidation, it is possible that an alternative pathway of NADH oxidation becomes operational under carbon starvation.

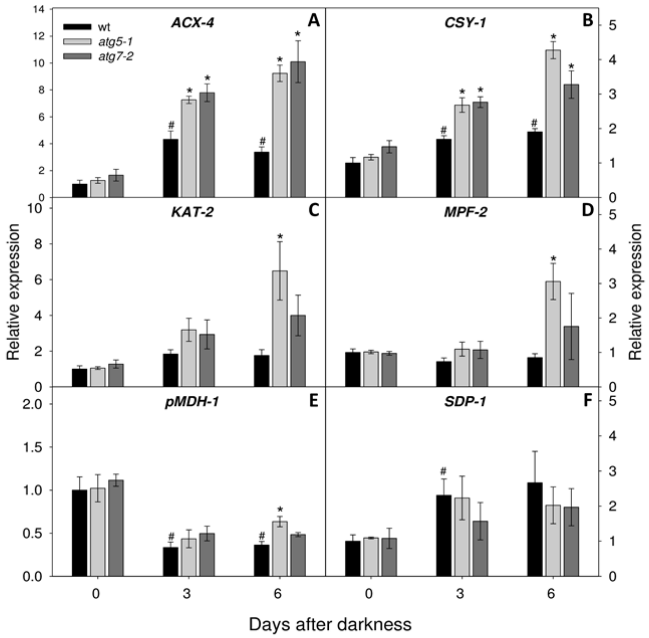

Figure 8 - Changes in transcript levels in WT and *atg* mutants during dark-induced senescence.
Transcript abundance is shown for genes associated with lipid catabolic pathways, including ACX-4 (A), CSY-1(B) KAT-2 (C), MPF-2 (D), pMDH-1 (E), SDP-1 (F). The y-axis values represent the expression level relative to the wild type (WT). Data were normalized with respect to the mean response calculated for the 0-d dark-treated leaves of the WT. Values presented are means ± SE of three independent biological replicates. An asterisk (*) indicates values that were determined by Student's t-test to be significantly different ($P < 0.05$) from the WT at each time point analyzed. A number sign (#) indicates values determined by Student's t-test to be significantly different ($P < 0.05$) from WT at 0d.

To investigate whether the reduced number of LDs is a result of the induction of catabolic pathways or impairment in biosynthesis, we next evaluated the expression of *SDP-1* gene. Despite being characterized as the primary lipase mediating LD catabolism in seeds, compelling evidence has suggested that *SDP-1* also operates in senescent and carbon-starved leaves (Fan et al., 2017, 2019). Indeed, an accumulation of *SDP-1* transcript levels was observed in WT plants during the early stages of darkness (Fig. 8F). Nonetheless, no significant difference in *SDP-1* transcript levels between WT plants and *atg5-1* and *atg7-2* was observed, suggesting that the reduced levels of LDs

are likely more related to the impairment of LD biogenesis rather than an induction of LD degradation pathways.

Altered FFA response of *atg* mutants under dark-induced senescence

Since autophagy deficiency altered cytosolic LD dynamics and β-oxidation pathways, we next evaluated if this response also affected the pool of free FA (FFA). Figure 9 shows that long-chain FFA (between 13C-21C chain length) are the more affected by both genotype and darkness, while no major changes were observed for very long-chain FFA (> 22C). Higher levels of 16:3, 18:1, 18:2, 18:3 in *atg5-1* and *atg7-2* genotypes under control conditions were observed, reinforcing the functional role of autophagy in basal lipid homeostasis. Upon darkness treatment, the levels of C18 and C20 FFAs were reduced, and unsaturated C16 accumulated in *atg5-1* and *atg7-2* mutants (Fig. 9). By contrast, WT plants presented an initial increase followed by later reduction of C16 and C18 FFAs except for 16:3 and 18:1 species FFAs, which were respectively, accumulated and reduced throughout darkness (Fig. 9). Although unsaturated C16 and C18 FAs are typical components of chloroplast membranes, only 16:3 is exclusively found in the thylakoid lipid MGDG in plant species (e.g. Arabidopsis), and it is, therefore, a chloroplast lipid marker (Ohlrogge et al., 1991; Kunz et al., 2009; Hölzl and Dörmann, 2019). Thus, the overall accumulation of 16:3 is in good agreement with the reduction of galactolipids observed under dark-induced senescence. Additionally, this result suggests that the rate of 16:3 release exceeds its channeling to LD and PG. The higher accumulation of 16:3 in *atg* mutants strengthens our claim that this disbalance is more intense when autophagy is disrupted.

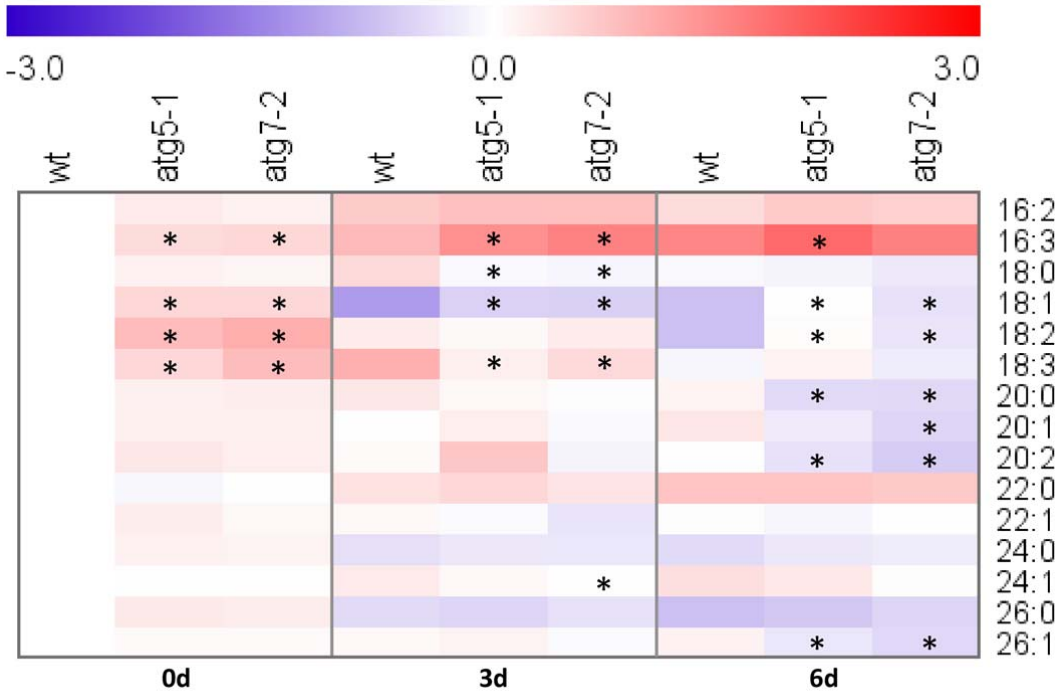

Figure 9- Changes in free Fatty Acid levels in WT and *atg* mutant plants under dark-induced senescence.

Values plotted are $\log_2$ fold change. Data were normalized to the mean response calculated for the 0-d dark treated leaves of the wild-type (WT). Values presented are means ± SE of five-six biological replicates per genotype; an asterisk (*) designate values that were determined by the Student's t-test to be significantly different ($P < 0.05$) from WT each time point analyzed.

Discussion

It is well established that plant autophagy plays a crucial role in the energetic metabolism mediating the supply of proteins and amino acids under carbon starvation conditions (Avin-Wittenberg et al., 2015; Barros et al., 2017; Hirota et al., 2018; McLoughlin et al., 2020). Furthermore, in both animals and yeast, autophagy is recognized as an important lipid catabolic pathway in starved cells (Singh et al., 2009). In plant leaves, growing evidence has highlighted the role of autophagy in managing cell lipid components and reserves (Avin-Wittenberg et al., 2015; McLoughlin et al., 2018,2020; Fan et al., 2019; Have et al., 2019). In fact, the lipid response of *atg* mutants under N starvation has been previously demonstrated (McLoughlin et al., 2018; Have et al., 2019). More recently, McLoughlin et al. (2020) reported extensive lipid alterations in maize *atg12* mutants submitted to carbon deprivation induced by short-term darkness. Here, we provide further evidence that autophagy broadly affects lipid and LD metabolism during dark-induced senescence in Arabidopsis. Notably, similarities and differences between the aforementioned studies and the findings reported here were

437 observed. The main points were summarized in Supplemental Figure S3, and they will
438 be further discussed throughout the text.

439 By performing a detailed lipidomics analysis, we revealed that autophagy widely
440 affects the lipid homeostasis of Arabidopsis during dark-induced senescence. The major
441 differences reported here are related to the *atg5-1* and *atg7-2* mutant plants,
442 characterized by a full inhibition of autophagy (Chung et al., 2010). By contrast, *atg9-4*,
443 which is characterized by a partial reduction of autophagy, presented an intermediary
444 impact on lipid metabolism that was more evident during the late stages of extended
445 darkness (Fig. 1 and Supplemental Figure S1). The fact that *atg9-4* did not cluster with
446 *atg5-1* and *atg7-2* implies that the lipid response is directly related to autophagy
447 intensity. Indeed, the characterization of Arabidopsis *ATG5* and *ATG7* knockout and
448 overexpression mutants showed a positive correlation between the level of autophagy
449 and seed FA content (Minina et al., 2018). We previously demonstrated that amino acid
450 catabolic pathways were less compromised in *atg9-4* mutants, contributing to its more
451 tolerant phenotype during dark-induced senescence (Barros et al., 2017). Additionally,
452 the limited reproductive phenotype of *atg* mutants is also dependent on autophagy
453 intensity since parameters related to seed and silique production were more
454 compromised in *atg* lines fully defective in autophagy (Barros et al., 2017). Taking into
455 account the fact that Arabidopsis is an oilseed (Li et al., 2006), the results reported here
456 and by others (Minina et al., 2018) suggest that the altered reproductive and carbon
457 starved phenotype of *atg* mutants is likely not only a consequence of impairment of
458 protein catabolic process but is also derived from an extensive reprogramming of lipid
459 metabolism.

460 The detailed analysis of the specific lipid classes revealed an altered lipid
461 phenotype in mutants lacking autophagy under non-stress conditions. These differences
462 are mostly attributed to galactolipids and the phospholipids PC and PE, whereas minor
463 differences were observed for TAGs (Figs 2, 3, and 4). The galactolipids MGDG and
464 DGDG are prevalent in the chloroplast envelope and the thylakoid membrane (Hölzl
465 and Dörmann, 2019). By contrast, PC and PE are highly abundant in the plasma
466 membrane, mitochondrial membrane, and endoplasmic reticulum (Liu et al., 2015).
467 Hence, the high levels of PC and low levels of MGDG and DGDG reveal an imbalance
468 of cytosolic and plastidial membrane lipids in *atg5-1* and *atg7-2* mutants under normal
469 growth conditions. Similar results were previously reported in Arabidopsis *atg5*
470 mutants, which displayed a general alteration of phospholipid levels under non-stressful

conditions (Have et al., 2019). The accumulation of lipid-breakdown products in maize *atg12* mutants also suggested an induced turnover of membrane components under normal growth conditions (McLoughlin et al., 2018, 2020). In addition, Fan et al., 2019 reported that the disrupted membrane lipid turnover in *atg* mutants affected TAG synthesis. The TAG profile detailed here reveals that only specific TAG species are reduced in *atg5-1,* and *atg7-2* mutants under normal growth conditions, which seems to contribute to the low total TAG content previously reported.

Collectively, our results support the notion that, beyond the role of autophagy in basal lipid metabolism, autophagy is clearly required for lipid remodeling under starvation conditions in Arabidopsis. Upon exposure to extended darkness, PC metabolism is broadly rearranged, presenting different patterns of accumulation and reduction (Fig. 2). In general, the majority of 32C and 34C PC species increases, whereas 36C and 38C declines upon darkness (Fig. 2). However, an altered response of PC accumulation and degradation was observed in *atg* mutants. The turnover of membrane lipids is a recognized aspect of plant senescence in general (Troncoso-Ponce et al., 2013). It seems that the disruption of autophagy leads to a differential degradation rate of membrane lipid components, most likely affecting the supply of FAs to sustain other cellular processes, including respiration. Alteration of PE levels was also observed in *atg* mutants under our experimental conditions (Fig. 2). Noteworthy, PE is an essential component of ATG8 conjugation during autophagosome membrane biogenesis (Soto-Burgo et al., 2018; Barros et al., 2020). The less accentuated reductions and accumulation of several PE species (PE 36:4, 36:3(1), 38:2, 36:5, 38:3) in *atg* mutants might be related to the disrupted usage and recycling of these molecules for autophagosome biogenesis, as previously suggested (Avin-Wittenberg et al., 2015; Have et al., 2019).

Apart from changes in the extra-plastidial phospholipids, *atg7-2* and *atg5-1* mutants also presented intense degradation of chloroplastic MGDG and DGDG during dark-induced senescence (Fig. 5). This data is consistent with the hypersensitive phenotype marked by chloroplast dismantling observed in *atg* mutants submitted to dark-induced senescence (Thompson et al., 2005; Phillips et al., 2008; Barros et al., 2017). Accordingly, autophagy has been characterized to mediate the degradation of chloroplast proteins by different selective processes (Ishida et al., 2008; Wada et al., 2009; Michaeli et al., 2014; Izumi et al., 2017; Nakamura et al., 2018). This fact aside, the results shown here reinforce the hypothesis that other pathways likely mediate the

degradation of chloroplast lipid components in carbon-starved plants and that they are likely to be more active when autophagy is absent. Moreover, this response is not restricted to carbon limitation, as similar results were reported in both Arabidopsis and maize *atg* mutants under low-nitrogen conditions (Supplemental Figure S3) (McLoughlin et al., 2018; Have et al., 2019).

The breakdown of membrane lipid components releases FFAs for further oxidation in peroxisomes. The overaccumulation of FFAs is detrimental to the plant cell. Consequently, FFAs are first incorporated as neutral lipids, to then be directed to peroxisomal FA catabolic pathways (Fan et al., 2017). TAGs stored in LDs are not abundant in leaf mesophyll cells. However, their number substantially increases under abiotic conditions and developmental senescence (Pyc et al., 2017; Yang et al., 2018). In agreement with this, we observed a transient LD accumulation after 3d of darkness in WT plants. In addition, a marked increase of highly unsaturated TAG levels was observed after 3d of darkness in WT (Fig. 3). Despite an increase of some FFA species after 3d of darkness, this increase was not overloaded to result in a lipotoxic effect since WT plants present favorable performance under dark-induced senescence (Barros et al., 2017). Indeed, the pattern of initial accumulation and later reduction of FFA 16:2, 18:0, 18:2, 18:3 was similar to the observed for TAG and LD (Figs. 4, 5 and 9), suggesting a dynamic equilibrium between membrane consumption, lipid reserve formation, and FA utilization in WT plants. By contrast, not only LD accumulation was disrupted in *atg5-1* and *atg7-2* mutants, but they also showed lower levels of unsaturated TAGs and higher accumulation of plastidial FFA 16:3 after 3d and 6d of darkness. Collectively, these results demonstrate that autophagy is required for the proper mobilization of chloroplast lipids destined for cytosolic LD biosynthesis in Arabidopsis starved cells. A recent study of maize *atg12* mutants subjected to carbon deprivation reported distinct LD dynamics (McLoughlin et al., 2020). It was observed that *atg12* mutants contained more cytoplasmic LD under normal growth conditions. In individually darkened leaves, LD numbers were not affected in WT and only slightly reduced in the *atg12* mutant. A possible explanation for this discrepancy may stem from the experimental systems utilized. While McLoughlin et al. (2020) analyzed individually darkened leaves of maize, we examined Arabidopsis in a whole plant darkening system. Plants have divergent metabolic strategies in response to different darkening treatments (Law et al., 2018). It has been postulated that individually darkened leaves still receive sugars from other parts of the plant during short-term dark periods. However, the lipid catabolic

539 response is not activated as long as carbohydrates are available, which likely affects LD
540 dynamics (Kunz et al., 2009; Law et al., 2018). Not only LD responses diverge
541 according to the darkness treatment imposed, but the results reported until now also
542 open new avenues regarding contrasting LD responses in different plant species.

543 In Arabidopsis, autophagy operates in the mobilization of FAs from organelle
544 membranes to TAG synthesis under normal growth conditions (Fan et al., 2019). The
545 same study stated that autophagy has no influence on TAG formation during darkness,
546 but instead operates in LD degradation by lipophagy mechanism. Despite that, general
547 TAG accumulation was observed in *atg* mutants after 6d of darkness, which was not
548 accompanied by cytosolic LD accumulation (Figs 4 and 5). Nonetheless, caution must
549 be taken when comparing the results obtained here with previous findings (Fan et al.,
550 2019) due to the differences of the genotypes analyzed (Barros et al., 2020). Thus,
551 although Fan et al. (2019) demonstrated the existence of lipophagy in different mutant
552 backgrounds, we analyzed plants solely lacking autophagy. When considered together,
553 our results, coupled with the results from Fan and colleagues, highlight the potential
554 role of autophagy as a versatile player in LD metabolism, particularly in starved cells.

555 Beyond the LDs in the cytosol, PG serve as subcompartments for lipid
556 biosynthesis and storage in chloroplasts (Rottet et al., 2015; van Wijk and Kessler,
557 2017). The analysis of PG-related genes indicates a marked activation of PG
558 metabolism in *atg5-1* and *atg7-2* mutants during dark-induced senescence (Fig. 6). In
559 agreement with that, we observed the presence of large PG in chloroplasts of *atg5-1*
560 mutants under extended darkness conditions (Fig. 7A-C). On the other hand, a reduced
561 abundance of the PG core protein FBN1a was observed in *atg* mutants after 6d of
562 darkness (Fig. 7D and Supplemental Figure S2). It is noteworthy that fibrillin proteins,
563 localized on the PG surface, were proposed to play both structural and protection roles
564 in chloroplast, preventing the PG coalescence and delaying thylakoid disintegration
565 (Austin et al., 2006; Ytterberg et al., 2006; Simkin et al., 2007; Singh et al., 2011; Rottet
566 al., 2015). It is tempting to suggest, therefore, that the reduction of FBN1a protein can
567 be associated with the large size of PG as well as chloroplast sensitive phenotype in *atg*
568 mutants in response to dark-induced senescence.There is a strong correlation between
569 thylakoid dismantling and supersizing of PG during senescence, which is likely
570 associated with the massive deposit of FAs and phytol, released from chloroplast
571 degradation (Lippold et al., 2012; Besagni et al., 2013; Rottet et al., 2015; van Wijk and
572 Kessler, 2017). In light of this, we also verified an increase of *PPH* transcript in *atg5-1*

and *atg7-2* mutants compared to WT under darkness (Fig. 6D). It seems reasonable to assume that both the products from the degradation of chlorophyll (Barros et al., 2017) and chloroplast membranes are funnelled for PG formation in *atg* mutants submitted to extended darkness (Fig. 3,7,10). This response can be presumed as a strategic mechanism preventing the accumulation of lipotoxic intermediaries. Collectively, our results imply that the disruption of autophagy triggers a differential response prompting PG rather than cytosolic LD formation under dark-induced senescence. Nonetheless, whether PG can be remobilized to provide lipid-derived energetic substrates remains to be further investigated.

It is already known that, during extended darkness, FAs are oxidized by β-oxidation, generating acetyl-CoA that, combined with oxaloacetate, produces citrate to be exported to mitochondria for ATP generation (Kunz et al., 2009). To further understand whether the released membrane lipid components were channeled to the maintenance of the energetic status, we paid particular attention to the transcriptional activation of lipid oxidation pathways. Our results show an up-regulation of peroxisomal genes in plants with disrupted autophagy after 6d and 9d of darkness (Fig. 8). Notably, the transcriptional induction of β-oxidation has been correlated to mitochondrial activity in darkened leaves (Law et al., 2018). Interestingly, the same *atg* mutants exhibited higher rates of respiration and an elegant metabolic reprogramming under carbon starvation conditions (Avin-Winttenberg et al., 2015; Barros et al., 2017).

Autophagy also plays a role in peroxisome quality control by the selective degradation of damaged peroxisomes, a process known as pexophagy (Marshall and Vierstra, 2018). The accumulation of peroxisome-related transcripts/proteins in *atg* mutants has been reported lately, and it can represent both activation of peroxisomal metabolism or accumulation of oxidized peroxisome (Supplemental Figure S3) (McLoughlin et al., 2018, 2020; Have et al.,2019). Specifically, under carbon starvation conditions, the enrichment of peroxisomal proteins was followed by an increase of glyoxysomal proteins (McLoughlin et al., 2020). This response suggests that peroxisomes are most likely converted to glyoxysomes to sustain high activation of FA ß-oxidation pathways during starvation conditions (McLoughlin et al., 2020). The induction of peroxisomal pathways reported here is positively correlated with the high levels of plastidial FFAs in *atg* mutants, which can be interpreted as a response to control FFA levels concomitantly with energy production. When taken together with our work, these studies suggest that the primary metabolism of *atg* mutants is not only

607 rearranged for amino acid catabolism but is also possibly involved in supporting lipid
608 oxidation pathways. In light of this, further studies are clearly required (*i*) to investigate
609 whether the disruption of LD dynamics and differential membrane recycling of *atg*
610 mutants impact the supply of lipid substrates for FA oxidation pathways and (*ii*) to
611 characterize the function of autophagy under a range of environmental stresses during
612 this process.
613
614 **Conclusions**
615 In the current work, we present compelling evidence regarding the importance of
616 autophagy to lipid homeostasis in Arabidopsis leaves. During carbon starvation, the
617 products of organellar membrane recycling are channeled to cytosolic LD production.
618 This enables the balance of FA production and turnover. The functional lack of
619 autophagy impacts proper membrane mobilization and activates a general chloroplast
620 lipid degradation program while failing to produce cytosolic LDs. Nonetheless, the
621 products of chloroplast membrane dismantling are possibly channeled to PG generation
622 in *atg* mutants chloroplasts (Fig. 10). We postulate that the increased activation of
623 peroxisomal lipid catabolic pathways is part of a complex metabolic response to
624 catabolize the FFAs released from chloroplast dismantling, and possibly, from PG
625 mobilization. Although our results highlight novel insights regarding the role of
626 autophagy in lipid metabolism, they certainly underestimate the complex crosstalk
627 between autophagy, peroxisome, mitochondria, and the endoplasmic reticulum. An
628 investigation of the interplay involving autophagy, membrane recycling, and organellar
629 maintenance is required to fully understand the implications of autophagy for the
630 regulation of lipid reserve dynamics and energy homeostasis. The combined results
631 presented here are of potential application for the breeding of crops with a higher yield,
632 increased resilience, and it seems reasonable to assume that there is a timely need to
633 accelerate our understanding of the mechanisms controlling autophagy and associated
634 processes in response to environmental conditions.
635
636

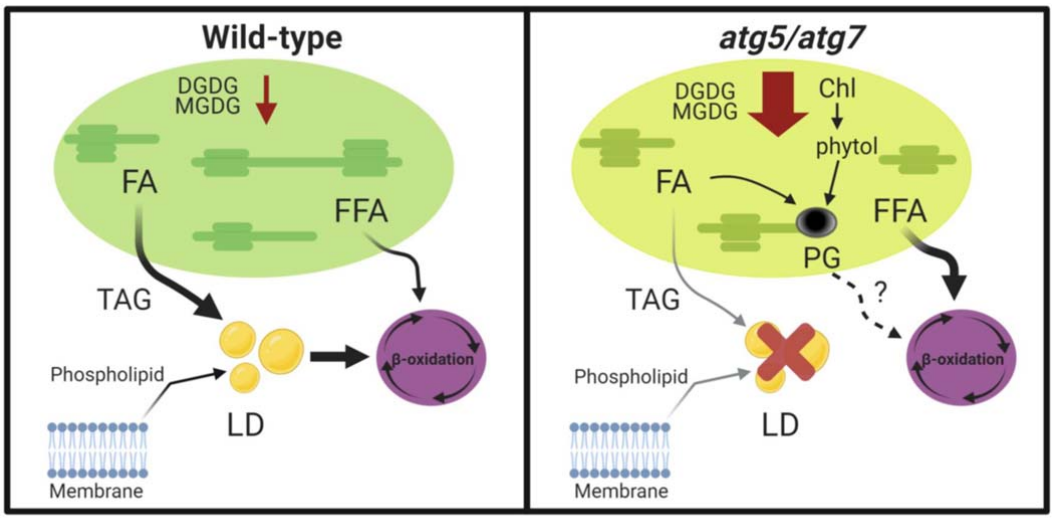

Figure 10 - Schematic model of lipid remodeling response of *atg* mutants during extended darkness.
Under extended darkness, the plastidial and extraplastidial membranes, composed by MGDG/DGDG and phospholipids, respectively, are degraded, releasing FAs to be stored as TAGs in LD in the cytosol. LDs and transient FFA donate substrates for β-oxidation in peroxisomes. Meanwhile, in *atg* mutants, there is a substantial degradation of chloroplast lipids, while the production of cytosolic LDs is impaired. Part of the released plastidial FAs, together with phytol derived from chlorophyll degradation, are channeled to the production of PG in the chloroplast. β-oxidation pathways are highly induced to consume overloaded plastidial FFA and, possibly, PG lipids (question mark). Abbreviations: Digalactosyldiacylglycerol (DGDG); Fatty acids (FA); Free Fatty Acids (FFA); Lipid Droplet (LD); Monogalactosyldiacylglycerol (MGDG).

Methods

Plant Material and Dark Treatment

All *Arabidopsis thaliana* (L.) Heynh plants used in this study were of the Columbia ecotype (Col-0). The T-DNA mutant lines *atg9-4* (SALK_145980) (Shin et al., 2014), *atg5-1* (SAIL_129B079) (Yoshimoto et al., 2009), *atg7-2* (GK-655B06) (Hofius et al., 2009) were used in this study. Seeds were surface-sterilized and imbibed for 4 days at 4°C in the dark on 0.7% (w/v) agar plates containing half-strength Murashige and Skoog (MS) media (Sigma-Aldrich; pH 5.7). Seeds were subsequently germinated and grown at 22°C under short-day conditions (8 h light/16 h dark), 60% relative humidity with 150 µmol photons m^{-2} s^{-1}. For dark treatments and subsequent induction of dark-induced senescence, 10- to 14-day-old seedlings were transferred to soil and then grown at 22°C under short-day conditions (8 h light/16 h dark). Four-week-old plants were transferred to darkness in the same growth cabinet. Whole rosettes of two different plants representing an independent replicated by genotype were harvested at intervals of 0, 3, 6, 9 days after transition to darkness. At least five biological replicates of each genotype were obtained. They were immediately frozen in liquid nitrogen and stored at –80°C until further analysis.

656 **Visualization and Analysis of LDs**

657 To visualize LDs in Arabidopsis leaves, LDs were stained with BODIPY
658 493/503 (Invitrogen; from 4 mg/mL stock in DMSO). The sixth rosette leaf of 4-week-
659 old plants was used for LD visualization and analysis. Leaf discs were stained with
660 BODIPY solution (2μg/mL) in the dark and under vacuum for 10 min. Confocal images
661 were acquired using the FV-1200 confocal microscope (Olympus, Japan) with a
662 60X/1.42 oil immersion objective. Excitation was performed at 488nm, and emission
663 was collected between 500-540nm for BODIPY 493/503 and 650-750nm for the
664 chlorophyll autofluorescence. The LD number was quantified using ImageJ (Schneider
665 et al., 2012). Z-stack series of three images from four plants for each genotype were
666 used for the quantification of LDs.

667

668 **Lipid Profiling and Free Fatty Acid Analysis**

669 Lipids and natural endogenic free fatty acids were extracted from six biological
670 replicates using the MTBE method described by Salem et al. (2016). Vacuum-dried
671 organic phases were processed using ultra-performance liquid chromatography (on a C8
672 reverse-phase column) coupled with Fourier transform mass spectrometry (exactive
673 mass spectrometer; Thermo Fisher Scientific) in positive and negative ionization modes.
674 The free fatty acid were analysed using ultra-performance liquid chromatography
675 (Waters, Acquity I Class System) coupled with mass spectrometer (Q-Exactive Thermo
676 Fisher Scientific, H-ESI). Processing of chromatograms, peak detection, and integration
677 were performed using REFINER MSH 10 (GeneData). Processing of mass spectrometry
678 data included the removal of the fragmentation information, isotopic peaks, and
679 chemical noise. Selected features were annotated using an in-house lipid database
680 (Lapidot-Cohen et al., 2020). Five-six biological replicates were used for the analysis.

681

682 **Expression analysis by RT-PCR**

683 Total RNA was isolated using TRIzol reagent (Ambion, Life Technology)
684 according to the manufacturer's recommendations. The total RNA was treated with
685 TURBO DNA-free kit (Invitrogen). The integrity of the RNA was checked on 1% (w/v)
686 agarose gels, and the concentration was measured using a Nanodrop spectrophotometer.
687 Finally, 1 μg of total RNA was reverse transcribed with SensiFAST cDNA Synthesis
688 Kit (Bioline) according to the manufacturer's recommendations. Real-time PCR
689 reactions were performed in a 384-well microlitre using SensiFAST SYBR® No-ROX

690 Kit (Bioline). The primers used here were designed using the open-source program
691 QuantPrime-qPCR primer designed tool (Arvidsson et al., 2008) and are described in
692 Table S2. The transcript abundance was calculated by the standard curves of each
693 selected gene and normalized using the constitutively expressed genes ACTIN
694 (AT2G37620). Three biological replicates were processed for each experimental
695 condition.
696
697 **Transmission Electron Microscopy**
698 Small pieces of leaves were cut and fixed in 3% Glutaraldeyde in 0.1M Cacodylate
699 buffer (pH 7.4) 10 hours at room temperature in a desiccator and then transferred to
700 40°C for the continuation of fixation overnight. The tissues were washed in cacodylate
701 buffer and postfixed and stained with 2% osmium tetroxide, 1.5% potassium
702 ferricyanide in 0.1M cacodylate buffer for 2 hours. Tissues were then washed in
703 cacodylate buffer and dehydrated through a graded series of ethanol treatments for 10
704 min each step, followed by 100% anhydrous ethanol 3 times, 20 min each, and
705 propylene oxide 2 times, 10 min each. The tissues were infiltrated with increasing
706 concentrations of Agar 100 resin in propylene oxide for 16 hours each step. The tissues
707 were embedded in fresh resin in a 600°C oven for 48 hours. Ultrathin sections,
708 approximately 80 nm thick, were cut on a Leica Reichert Ultracut S microtome,
709 collected onto 200 Mesh carbon-formvar coated copper grids, and stained with Uranyl
710 acetate followed by Reynold's Lead Citrate for 10 min. The sections were examined
711 using Tecnai 12 TEM 100kV (Phillips, Eindhoven, the Netherlands) equipped with
712 MegaView II CCD camera and Analysis® version 3.0 software (SoftImaging System
713 GmbH, Münstar, Germany).
714
715 **Immunoblot Analyses**
716 Plant leaf tissue (~100 mg) was ground in liquid nitrogen, and total proteins
717 were extracted using a protein extraction buffer previously described (Gruis et al.,
718 2002). After the addition of buffer, centrifuged for 15 min at 20,000g; supernatants
719 were collected, and samples were incubated immediately for 10 min at 100°C, vortexed,
720 and samples were adjusted in SDS-PAGE sample buffer (Laemmli, 1970). Total
721 proteins were separated by SDS-PAGE and transferred to a polyvinylidene difluoride
722 membrane (GE Healthcare Life science). Equal loading was validated using Coomassie
723 Brilliant Blue staining of the membrane. For immunodetection, antibodies raised against

FBN1a (Agrisera; AS06116) was used in combination with horseradish peroxidase-conjugated goat anti-rabbit antibody (Sigma; ab920)

Statistical analyses

The experiments were conducted in a completely randomized design with 3-6 replicates of each genotype. Data were statistically examined using analysis of variance and tested for significant ($P < 0.05$) differences using Student's *t* tests from algorithm embedded into Microsoft Excel. Principal component analysis (PCA) was performed to reduce the dataset and identify the variables that best explained the highest proportion of total variance using Metaboanalyst 4.0, an open-source web-based tool for metabolomics data analysis (Chong et al., 2019).

Accession Numbers

The Arabidopsis Genome Initiative locus numbers for the main genes discussed in this article are as follows: *ATG5* (At5g17290), *ATG7* (At5g45900), and *ATG9* (At2g31260).

Supplemental Data

The following supplemental materials are available.

Supplemental Figure S1: Lipid response of *atg* mutants throughout dark-induced senescence. Principal component analysis (PCA) was performed using the lipid data of *atg5-1, atg7-2, atg9-4* and wild type (WT) genotypes after 0 (0d), 3 (3d), (6d), and 9 (9d) days of dark treatment.

Supplemental Figure S2: Quantification of the FBN1a protein signal

Integrated density values for FBN1a were first normalized to loading control and then expressed as a percentage of the obtained value for the wild type (WT) at 0d. Data represent means ±SE; n= 3 biological replicates. An asterisk (*) indicates values that were determined by Student's t-test to be significantly different ($P < 0.05$) from the WT at each time point analyzed.

Supplemental Figure S3: Compared lipidomics of Arabidopsis and maize *atg* mutants under carbon and nitrogen starvation. General representation of the changes in Phospholipids, Galactolipds, Lipid Droplet number, and β-oxidation transcripts reported in Arabidopsis and maize under carbon starvation (this study; McLoughlin et al., 2020) and nitrogen starvation (McLoughlin et al., 2018; Have et al., 2019). The scheme does not take into consideration the experimental differences in these studies. Abbreviations-

PC: Phosphatidylcholine; PE-: Phosphatidylethanolamine; PG: phosphatidylglycerol; -C: Carbon starvation; -N: Nitrogen starvation

Supplemental Table S1: Summary of the main variables of the first three Principal Component (PC) of *atg* mutants and wild type (WT) genotypes after 0 and 6 days of dark treatment. The contribution of which PC is showed as cumulative variance (CV).

Supplemental Table S2: Primers used in the RT-PCR analyses performed in this study

Supplemental Table S3: Relative lipid content of leaves of Arabidopsis knockout mutants *atg5-1, atg7-2, atg9-4,* and wild type (WT) after 0, 3, 6, and 9 days of dark treatment

Supplemental Table S4: Variables of the first three Principal Component (PC) of *atg* mutants and wild type (WT) genotypes after 0 and 6 days of dark treatment

ACKNOWLEDGEMENTS

We thank Prof. Oren Ostersetzer-Biran from The Hebrew University of Jerusalem for providing the facilities allowing transcript analysis, as well as Corinne Best and Sofia Shevtsov, for their assistance with qPCR analyses. We also thank Dr. Naomi Melamed-Book and Dr. Yael Friedmann from the microscopy core facility at The Hebrew University's Life Science core facility for her technical support with confocal and EM analysis. We also thank Prof. Zack Adam from The Hebrew University of Jerusalem for providing us with the anti- FBN1a antibody.

FIGURE CAPTIONS

Figure 1 - Differential lipid response of *atg* mutants under dark-induced senescence.

Principal component analysis (PCA) was performed using the lipid data obtained in samples from 4-week-old Arabidopsis plants immediately before lights were turned off (0 d) and after further treatment for 6d in darkness. Three loss-of-function mutants of the autophagy pathway, namely *atg5-1, atg7-2, atg9-4* and their respective wild type (WT) were analyzed.

Figure 2 - *atg* mutants present altered phospholipid levels under control and extended darkness conditions

Hierarchical clustering of (A) Phosphatidylcholine (PC) and (B) Phosphatidylethanolamine (PE). Values plotted are $\log_2$ fold change. Distances were measured by Pearson correlation using MeV 4.9.0 software. Data were normalized to the mean response calculated for the 0-d dark treated leaves of the wild type (WT). Values presented are means ± SE of five-six biological replicates per genotype; an asterisk (*) designates values that were determined by Student's t-test to be significantly different ($P < 0.05$) from WT at each time point analyzed.

Figure 3 - Chloroplast lipids are substantially reduced in *atg* mutants during dark-induced senescence

Monogalactosyldiacylglycerol (MGDG) and Digalactosyldiacylglycerol (DGDG) values plotted are $\log_2$ fold change. Data were normalized to the mean response calculated for the 0-d dark treated leaves of the wild type (WT). Values presented are means ± SE of five-six biological replicates per genotype; an asterisk (*) designate values that were determined by the Student's t-test to be significantly different ($P < 0.05$) from WT at each time point analyzed.

Figure 4 - Distinct accumulation of neutral lipids in *atg* mutants during dark-induced senescence

(A) Triacylglycerol (TAG) and (B) Diacylglycerol (DAG). Values plotted are $\log_2$ fold change. Data were normalized to the mean response calculated for the 0-d dark treated leaves of the wild type (WT). Values presented are means ± SE of five-six biological replicates per genotype; an asterisk (*) designates values that were determined by Student's t-test to be significantly different ($P < 0.05$) from WT each time point analyzed.

Figure 5 - Autophagy deficiency affects Lipid Droplet (LD) dynamics during dark-induced senescence

(A) Representative confocal images of LDs (BODIPY 493/503 fluorescence, false color (green) in wild type (WT), *atg5-1*, and *atg7-2* leaves. (B) Merged image of BODIPY and chloroplast autofluorescence (false color red). Images were collected at the same magnification and are projections of Z-stacks of 20 optical sections Bar = 10 µm (C) Number of total LDs per image area. The number of LDs was quantified by ImageJ as BODIPY-stained lipid area in 2D projections of Z-stacks of 3 images of four biological replicates per genotype and time point.

Figure 6 - PG related genes are up-regulated in *atg* mutants during dark-induced senescence

Transcript abundance is shown for genes associated with plastoglobuli (PG), including PES-1 (A), PES-2 (B), ABC1K7 (C), PPH (D). The y-axis values represent the gene expression level relative to the wild type (WT). Data were normalized with respect to the mean response calculated for the 0-d dark-treated leaves of the WT. Values presented are means ± SE of three independent biological replicates. An asterisk (*) indicates values that were determined by Student's t-test to be significantly different ($P < 0.05$) from the WT at each time point analyzed. A number sign (#) indicates values determined by Student's t-test to be significantly different ($P < 0.05$) from WT at 0d.

Figure 7: Autophagy disruption triggers altered PG response

(A) Transmission electron micrographs of leaves from 4-week-old Arabidopsis plants immediately before lights were turned off (0 d) and after further treatment for 7 days of darkness. Scale bar = 1 µm; Quantification of the number (B) and size (C) of plastoglobuli per chloroplasts (±SE, n= 6-7 chloroplasts of three independent cells); Analysis shown in A-C were performed in *atg5-1* and its respective wild type (WT). (D) Immunoblot analysis of the PG protein, FBN1a, was performed in leaves from 4-week-old Arabidopsis *atg5-1, atg7-2* and WT plants immediately before (0 d) and after further treatment for 3d and 6d in darkness. FBN1a protein display a predicted molecular mass to ~30-35 kD. The detection of a second lower band in the region of

30kD possibly corresponds to FBN1b protein (with high sequence similarity with FBN1a) as previously observed in Giacomelli et al., 2006; Matinis et al., 2013; 2014.

Figure 8 - Changes in transcript levels in WT and *atg* mutants during dark-induced senescence.

Transcript abundance is shown for genes associated with lipid catabolic pathways, including ACX-4 (A), CSY-1(B) KAT-2 (C), MPF-2 (D), pMDH-1 (E), SDP-1 (F). The y-axis values represent the expression level relative to the wild type (WT). Data were normalized with respect to the mean response calculated for the 0-d dark-treated leaves of the WT. Values presented are means ± SE of three independent biological replicates. An asterisk (*) indicates values that were determined by Student's t-test to be significantly different ($P < 0.05$) from the WT at each time point analyzed. A number sign (#) indicates values determined by Student's t-test to be significantly different ($P < 0.05$) from WT at 0d.

Figure 9- Changes in free Fatty Acid levels in WT and *atg* mutant plants under dark-induced senescence.

Values plotted are $\log_2$ fold change. Data were normalized to the mean response calculated for the 0-d dark treated leaves of the wild-type (WT). Values presented are means ± SE of five-six biological replicates per genotype; an asterisk (*) designate values that were determined by the Student's t-test to be significantly different ($P < 0.05$) from WT each time point analyzed.

Figure 10 - Schematic model of lipid remodeling response of *atg* mutants during extended darkness.

Under extended darkness, the plastidial and extraplastidial membranes, composed by MGDG/DGDG and phospholipids, respectively, are degraded, releasing FAs to be stored as TAGs in LD in the cytosol. LDs and transient FFA donate substrates for β-oxidation in peroxisomes. Meanwhile, in *atg* mutants, there is a substantial degradation of chloroplast lipids, while the production of cytosolic LDs is impaired. Part of the released plastidial FAs, together with phytol derived from chlorophyll degradation, are channeled to the production of PG in the chloroplast. β-oxidation pathways are highly induced to consume overloaded plastidial FFA and, possibly, PG lipids (question mark). Abbreviations: Digalactosyldiacylglycerol (DGDG); Fatty acids (FA); Free Fatty Acids (FFA); Lipid Droplet (LD); Monogalactosyldiacylglycerol (MGDG).

Parsed Citations

Araújo WL, Ishizaki K, Nunes-Nesi A, Larson TR, Tohge T, Krahnert I, Witt S, Obata T, Schauer N, Graham IA, Leaver CJ, Fernie AR (2010) Identification of the 2-hydroxyglutarate and isovaleryl-CoA dehydrogenases as alternative electron donors linking lysine catabolism to the electron transport chain of Arabidopsis mitochondria. Plant Cell 22: 1549-1563
Google Scholar: Author Only Title Only Author and Title

Araújo WL, Tohge T, Ishizaki K, Leaver CJ, Fernie AR (2011) Protein degradation: an alternative respiratory substrate for stressed plants. Trends Plant Sci 16: 489–498
Google Scholar: Author Only Title Only Author and Title

Avin-Wittenberg T, Bajdzienko K, Wittenberg G, Alseekh S, Tohge T, Bock R, Giavalisco P, Fernie AR (2015) Global analysis of the role of autophagy in cellular metabolism and energy homeostasis in Arabidopsis seedlings under carbon starvation. Plant Cell 27: 306–322
Google Scholar: Author Only Title Only Author and Title

Avin-Wittenberg T, Baluska F, Bozhkov PV, Elander PH, Fernie AR, Galili G, Hassan A, Hofius D, Isono E, Le Bars R et al (2018) Autophagy-related approaches for improving nutrient use efficiency and crop yield protection. J Exp Bot 69: 1335–1353
Google Scholar: Author Only Title Only Author and Title

Arvidsson S, Kwasniewski M, Riaño-Pachón DM, Mueller-Roeber B (2008) QuantPrime: a flexible tool for reliable high-throughput primer design for quantitative PCR. BMC Bioinformatics 9: 465
Google Scholar: Author Only Title Only Author and Title

Austin JR II, Frost E, Vidi PA, Kessler F, Staehelin LA (2006) Plastoglobules are lipoprotein subcompartments of the chloroplast that are permanently coupled to thylakoid membranes and contain biosynthetic enzymes. Plant Cell 18:1693–703
Google Scholar: Author Only Title Only Author and Title

Barros JAS, Cavalcanti JHF, Medeiros DB, Nunes-Nesi A, Avi-Wittenberg T, Fernie AR, Araújo WL (2017) Autophagy deficiency compromises alternative pathway 414 of respiration following energy deprivation. Plant Physiol 175: 62–76
Google Scholar: Author Only Title Only Author and Title

Barros JAS, Siqueira JAB, Cavalcanti JHF, Araújo WL, Avin-Wittenberg T (2020) Multifaceted Roles of Plant Autophagy in Lipid and Energy Metabolism. Trends Plant Sci. doi:10.1016/j.tplants.2020.05.004
Google Scholar: Author Only Title Only Author and Title

Besagni C, Kessler F (2013) A mechanism implicating plastoglobules in thylakoid disassembly during senescence and nitrogen starvation. Planta 237: 463-470
Google Scholar: Author Only Title Only Author and Title

Bhuiyan NH, Friso G, Rowland E, Majsec K, van Wijk KJ (2016) The plastoglobule-localized metallopeptidase PGM48 is a positive regulator of senescence in Arabidopsis thaliana. Plant Cell 28:3020–37
Google Scholar: Author Only Title Only Author and Title

Bréhélin C, Kessler F, van Wijk KJ (2007). Plastoglobules: Versatile lipoprotein particles in plastids. Trends Plant Sci. 12:260–266.
Google Scholar: Author Only Title Only Author and Title

Chong J, Wishart DS, Xia J (2019) Using MetaboAnalyst 4.0 for Comprehensive and Integrative Metabolomics Data Analysis. Curr. Protoc. Bioinform. 68: 1–128
Google Scholar: Author Only Title Only Author and Title

Chung T, Phillips AR, Vierstra RD (2010) ATG8 lipidation and ATG8-mediated autophagy in Arabidopsis require ATG12 expressed from the differentially controlled ATG12a and ATG12b loci. Plant J. 62:483–93
Google Scholar: Author Only Title Only Author and Title

Couso I, Perez-Perez ME, Martinez-Force E, Kim HS, He Y, Umen JG, Crespo JL (2017) Autophagic flux is required for the synthesis of triacylglycerols and ribosomal protein turnover in Chlamydomonas. J Exp Bot 69:1355–1367.
Google Scholar: Author Only Title Only Author and Title

Elander PH, Minina EA, Bozhkov PV (2018) Autophagy in turnover of lipid stores: trans-kingdom comparison. J. Exp. Bot. 69: 1301–1311.
Google Scholar: Author Only Title Only Author and Title

Fan J, Yan C, Zhang X, Xu C (2013) Dual role for phospholipid: diacylglycerol acyltransferase: Enhancing fatty acid synthesis and diverting fatty acids from membrane lipids to triacylglycerol in Arabidopsis leaves. Plant Cell 25: 3506–3518.
Google Scholar: Author Only Title Only Author and Title

Fan J, Yu L, Xu C (2017) A central role for triacylglycerol in membrane lipid breakdown, fatty acid b-oxidation, and plant survival under extended darkness. Plant Physiol. 174: 1517–1530.
Google Scholar: Author Only Title Only Author and Title

Fan J, Yu L, Xu CG (2019) Dual role of autophagy in lipid metabolism in Arabidopsis. Plant Cell 31: 1598–1613
Google Scholar: Author Only Title Only Author and Title

Gaude N, Bréhélin C, Tischendorf G, Kessler F, Dörmann P (2007) Nitrogen deficiency in Arabidopsis affects galactolipid composition

and gene expression and results in accumulation of fatty acid phytyl esters. Plant J. 49: 729–739.
Google Scholar: Author Only Title Only Author and Title

Giacomelli L, Rudella A, van Wijk KJ (2006) High light response of the thylakoid proteome in Arabidopsis wild type and the ascorbate deficient mutant vtc2-2. A comparative proteomics study. Plant Physiol 141: 685–701
Google Scholar: Author Only Title Only Author and Title

Gruis, D.F., Selinger, D.A., Curran, J.M., and Jung, R. (2002). Redundant proteolytic mechanisms process seed storage proteins in the absence of seed-type members of the vacuolar processing enzyme family of cysteine proteases. Plant Cell 14: 2863–2882
Google Scholar: Author Only Title Only Author and Title

Havé M, Luo J, Tellier F, Balliau T, Cueff G, Chardon F, Zivy M, Rajjou L, Cacas JL, Masclaux-Daubresse C (2019) Proteomic and lipidomic analyses of the Arabidopsis atg5 autophagy mutant reveal major changes in endoplasmic reticulum and peroxisome metabolisms and in lipid composition. New Phytologist 223: 1461–1477.
Google Scholar: Author Only Title Only Author and Title

Hirota T, Izumi M, Wada S, Makino A, Ishida H (2018) Vacuolar protein degradation via autophagy provides substrates to amino acid catabolic pathways as an adaptive response to sugar starvation in Arabidopsis thaliana. Plant Cell Physiol 59: 1363–458 1376
Google Scholar: Author Only Title Only Author and Title

Hofius D, Schultz-Larsen T, Joensen J, Tsitsigiannis DI, Petersen NH, Mattsson O, Jørgensen LB, Jones JD, Mundy J, Petersen M (2009) Autophagic components contribute to hypersensitive cell death in Arabidopsis. Cell 137: 773–783
Google Scholar: Author Only Title Only Author and Title

Hölzl G, Dörmann P (2019) Chloroplast lipids and their biosynthesis. Annu Rev Plant Biol 70: 51–81
Google Scholar: Author Only Title Only Author and Title

Hörtensteiner S, Kräutler B (2011) Chlorophyll breakdown in higher plants. Biochim. Biophys. Acta 1807: 977–988
Google Scholar: Author Only Title Only Author and Title

Ishida H, Yoshimoto K, Izumi M, Reisen D, Yano Y, Makino A, Ohsumi Y, Hanson MR, Mae T (2008) Mobilization of Rubisco and stroma-localized fluorescent proteins of chloroplasts to the vacuole by an ATG gene-dependent autophagic process. Plant Physiol 148: 142–155
Google Scholar: Author Only Title Only Author and Title

Ishizaki K, Larson TR, Schauer N, Fernie AR, Graham IA, Leaver CJ (2005) The critical role of Arabidopsis electron-transfer flavoprotein: Ubiquinone oxido reductase during dark-induced starvation. Plant Cell 17: 2587-2600
Google Scholar: Author Only Title Only Author and Title

Izumi M, Hidema J, Makino A, Ishida H (2013) Autophagy contributes to nighttime energy availability for growth in Arabidopsis. Plant Physiol 161: 1682-1693
Google Scholar: Author Only Title Only Author and Title

Izumi M, Ishida H, Nakamura S, Hidema J (2017) Entire photodamaged chloroplasts are transported to the central vacuole by Autophagy. Plant Cell 29: 377–394
Google Scholar: Author Only Title Only Author and Title

Kunz HH, Scharnewski M, Feussner K, Feussner I, Flügge UI, Fulda M, Gierth M (2009) The ABC transporter PXA1 and peroxisomal b-oxidation are vital for metabolism in mature leaves of Arabidopsis during extended darkness. Plant Cell 21: 2733–2749.Laemmli, U.K. (1970). Cleavage of structural proteins during the assembly of the head of bacteriophage T4. Nature 227: 680–685
Google Scholar: Author Only Title Only Author and Title

Lapidot-Cohen T, Rosental L, Brotman Y (2020) Liquid chromatography–mass spectrometry (LC-MS)-based analysis for lipophilic compound profiling in plants. Curr Protoc Plant Biol. 5 e20109. doi: 10.1002/cppb.20109
Google Scholar: Author Only Title Only Author and Title

Law SR, Chrobok D, Juvany M, Delhomme N, Lindén P, Brouwer B, Ahad A, Moritz T, Jansson S, Gardestrom P, Keech Olivier (2018) Darkened leaves use different metabolic strategies for senescence and survival. Plant Physiol 177: 132–150.
Google Scholar: Author Only Title Only Author and Title

Li F, Chung T, Vierstra RD (2014) AUTOPHAGY-RELATED11 plays a critical role in general autophagy and senescence-induced mitophagy in Arabidopsis. Plant Cell 26: 788-807.
Google Scholar: Author Only Title Only Author and Title

Li YH, Beisson F, Pollard M, Ohlrogge J (2006) Oil content of Arabidopsis seeds: The influence of seed anatomy, light and plantto-plant variation. Phytochemistry 67: 904–915.
Google Scholar: Author Only Title Only Author and Title

Lippold F, vom Dorp K, Abraham M, Hölzl G, Wewer V, Yilmaz JL, Lager I, Montandon C, Besagni C, Kessler F, Stymne S, Dörmanna P (2012) Fatty acid phytyl ester synthesis in chloroplasts of Arabidopsis. Plant Cell 24(5): 2001–14

Liu Y,Wang G,Wang X (2015) Role of aminoalcoholphosphotransferases 1 and 2 in phospholipid homeostasis in Arabidopsis. Plant Cell 27:1512–28
Google Scholar: Author Only Title Only Author and Title

Lundquist PK, Poliakov A, Bhuiyan NH, Zybailov B, Sun Q, van Wijk KJ (2012). The functional network of the Arabidopsis plastoglobule proteome based on quantitative proteomics and genome-wide coexpression analysis Plant Physiol.158: 1172-1192
Google Scholar: Author Only Title Only Author and Title

Marshall RS,Vierstra RD (2018) Autophagy: the master of bulk and selective recycling Annu. Rev. Plant Biol. 69: 173-208
Google Scholar: Author Only Title Only Author and Title

Martinis J, Glauser G, Valimareanu S, Kessler F (2013) A chloroplast ABC1-like kinase regulates vitamin E metabolism in Arabidopsis. Plant Physiol 162: 652–662
Google Scholar: Author Only Title Only Author and Title

Martinis J Glauser G Valimareanu S Stettler M Zeeman SC Yamamoto H Shikanai T Kessler F (2014) ABC1K1/PGR6 kinase: a regulatory link between photosynthetic activity and chloroplast metabolism. Plant Journal 77:269–283Masclaux-Daubresse C, d'Andrea S, Bouchez I, Cacas J-L (2020). Reserve lipids and plant autophagy. J Exp Bot. doi.org/10.1093/jxb/eraa082
Google Scholar: Author Only Title Only Author and Title

McLoughlin F, Augustine RC, Marshall RS, Li F, Kirkpatrick LD, Otegui MS, Vierstra RD (2018) Maize multi-omics reveal roles for autophagic recycling in proteome remodelling and lipid turnover. Nature Plants 4: 1056–1070.
Google Scholar: Author Only Title Only Author and Title

McLoughlin F, Marshall RS, Ding X, Chatt EC, Kirkpatrick LD, Augustine RC, Li F, Otegui MS, Vierstra RD (2020) Autophagy Plays Prominent Roles in Amino Acid, Nucleotide, and Carbohydrate Metabolism During Fixed-carbon Starvation in Maize. Plant Cell. DOI: 10.1105/tpc.20.00226
Google Scholar: Author Only Title Only Author and Title

Michaeli S, Honig A, Levanony H, Peled-Zehavi H, Galili G (2014) Arabidopsis ATG8-INTERACTING PROTEIN1 is involved in autophagy-dependent vesicular trafficking of plastid proteins to the vacuole. Plant Cell 26: 4084–4101
Google Scholar: Author Only Title Only Author and Title

Minina EA, Moschou PN, Vetukuri RR, Sanchez-Vera V, Cardoso C, Liu Q, Elander PH, Dalman K, Beganovic M, Yilmaz JL, Marmon S, Shabala L, Suarez MF, Ljung K, Novák O, Shabala S, Stymne S, Hofius D, Bozhkov PV (2018) Transcriptional stimulation of rate-limiting components of the autophagic pathway improves plant fitness. J Exp Bot 69: 1415–1432.
Google Scholar: Author Only Title Only Author and Title

Muthan B, Roston RL, Froehlich JE, Benning C (2013) Probing Arabidopsis chloroplast diacylglycerol pools by selectively targeting bacterial diacylglycerol kinase to suborganellar membranes. Plant Physiol. 163: 61–74.
Google Scholar: Author Only Title Only Author and Title

Nakamura S, Hidema J, Sakamoto W, Ishida H, Izumi M (2018) Selective elimination of membrane-damaged chloroplasts via microautophagy. Plant Physiol. 177: 1007–1026.
Google Scholar: Author Only Title Only Author and Title

Nguyen TB, Louie SM, Daniele JR, Tran Q, Dillin A, Zoncu R, Nomura DK, Olzmann, JA (2017) DGAT1-dependent lipid droplet biogenesis protects mitochondrial function during starvation-induced autophagy. Dev. Cell 42: 9–21
Google Scholar: Author Only Title Only Author and Title

Ohlrogge JB, Browse J, Somerville CR (1991) The genetics of plant lipids. Biochim. Biophy. Acta 1082: 1–26.
Google Scholar: Author Only Title Only Author and Title

Otegui MS, Noh YS, Martínez DE, Vila Petroff MG, Andrew Staehelin L, Amasino RM (2005) Senescence-associated vacuoles with intense proteolytic activity develop in leaves of Arabidopsis and soybean. Plant J 41: 831–844
Google Scholar: Author Only Title Only Author and Title

Phillips AR, Suttangkakul A, Vierstra RD (2008) The ATG12-conjugating enzyme ATG10 is essential for autophagic vesicle formation in Arabidopsis thaliana. Genetics 178: 1339–1353
Google Scholar: Author Only Title Only Author and Title

Pracharoenwattana I, Cornah JE, Smith SM (2007) Arabidopsis peroxisomal malate dehydrogenase functions in b-oxidation but not in the glyoxylate cycle. Plant J 50: 381–390
Google Scholar: Author Only Title Only Author and Title

Pugkaew W, Meetam M, Ponpuak M, Yokthongwattana K, Pokethitiyook P (2017) Role of autophagy in triacylglycerol biosynthesis in Chlamydomonas reinhardtii revealed by chemical inducer and inhibitors. J. Appl. Phycol. 30: 15–22.
Google Scholar: Author Only Title Only Author and Title

Pyc M, Cai Y, Greer MS, Yurchenko O, Chapman KD, Dyer JM, Mullen RT (2017) Turning over a new leaf in lipid droplet biology. Trends Plant Sci 22: 596–609
Google Scholar: Author Only Title Only Author and Title

Rambold AS, Cohen S, Lippincott-Schwartz J (2015) Fatty acid trafficking in starved cells: Regulation by lipid droplet lipolysis, autophagy, and mitochondrial fusion dynamics. Dev. Cell 32: 678–692.
Google Scholar: Author Only Title Only Author and Title

Rey P, Gillet B, R¨omer S, Eymery F, Massimino J (2000) Over-expression of a pepper plastid lipid-associated protein in tobacco leads to canges in plastid ultrastructure and plant development upon stress. Plant J. 21:483–94
Google Scholar: Author Only Title Only Author and Title

Rottet S, Besagni C, Kessler F (2015) The role of plastoglobules in thylakoid lipid remodeling during plant development. Biochim. Biophys. Acta 1847: 889–899
Google Scholar: Author Only Title Only Author and Title

Salem MA, Juppner J, Bajdzienko K, Giavalisco P (2016) Protocol: a fast, comprehensive and reproducible one-step extraction method for the rapid preparation of polar and semi-polar metabolites, lipids, proteins, starch and cell wall polymers from a single sample. Plant Methods 12: 45.
Google Scholar: Author Only Title Only Author and Title

Schneider CA, Rasband WS, Eliceiri KW (2012) NIH Image to ImageJ: 25 years of image analysis. Nat. Methods 9: 671–675.
Google Scholar: Author Only Title Only Author and Title

Schwarz V, Andosch A, Geretschläger A, Affenzeller M, Lütz-Meindl U (2017) Carbon starvation induces lipid degradation via autophagy in the model alga Micrasterias. J Plant Physiol 208:115–127.
Google Scholar: Author Only Title Only Author and Title

Shin KD, Lee HN, Chung T (2014) A revised assay for monitoring autophagic flux in Arabidopsis thaliana reveals involvement of AUTOPHAGY-RELATED9 in autophagy. Mol Cells 37: 399–405
Google Scholar: Author Only Title Only Author and Title

Simkin AJ, Gaffe J, Alcaraz JP, Carde JP, Bramley PM (2007). Fibrillin influence on plastid ultrastructure and pigment content in tomato fruit. Phytochemistry 68:1545–56

Singh R, Kaushik S, Wang Y, Xiang Y, Novak I, Komatsu M, Tanaka K, Cuervo AM, Czaja MJ (2009) Autophagy regulates lipid metabolism. Nature 458: 1131-1135
Google Scholar: Author Only Title Only Author and Title

Singh DK, McNellis TW (2011) Fibrillin protein function: the tip of the iceberg? Trends Plant Sci. 16:432–41
Google Scholar: Author Only Title Only Author and Title

Soto-Burgos J, Zhuang X, Jiang L, Bassham DC (2018) Dynamics of autophagosome formation. Plant Physiol. 176: 219–229.
Google Scholar: Author Only Title Only Author and Title

Testerink C, Munnik T (2011) Molecular, cellular, and physiological responses to phosphatidic acid formation in plants. J. Exp. Bot. 62: 2349–2361
Google Scholar: Author Only Title Only Author and Title

Thompson AR, Doelling JH, Suttangkakul A, Vierstra RD (2005) Autophagic nutrient recycling in Arabidopsis directed by the ATG8 and ATG12 conjugation pathways. Plant Physiol 138: 2097-2110
Google Scholar: Author Only Title Only Author and Title

Tran QG, Yoon HR, Cho K, Lee SJ, Crespo JL, Ramanan R, Kim HS (2019) Dynamic Interactions between Autophagosomes and Lipid Droplets in Chlamydomonas reinhardtii. Cells: 8:992
Google Scholar: Author Only Title Only Author and Title

Troncoso-Ponce MA, Cao X, Yang Z,Ohlrogge JB (2013) Lipid turnover during senescence. Plant Sci 205-206: 13–19
Google Scholar: Author Only Title Only Author and Title

van Wijk KJ, Kessler F (2017) Plastoglobuli: Plastid microcompartments with integrated functions in metabolism, plastid developmental transitions, and environmental adaptation. Annu Rev Plant Biol 68: 253–289
Google Scholar: Author Only Title Only Author and Title

Wada S, Ishida H, Izumi M, Yoshimoto K, Ohsumi Y, Mae T, Makino A (2009) Autophagy plays a role in chloroplast degradation during senescence in individually darkened leaves. Plant Physiol 149: 885–893
Google Scholar: Author Only Title Only Author and Title

Wang X, Devaiah SP, Zhang W, Welti R (2006) Signaling functions of phosphatidic acid. Prog Lipid Res. 5: 250–78
Google Scholar: Author Only Title Only Author and Title

Wood WHJ, Barnett SFH, Flannery S, Hunter CN, Johnson MP (2019) Dynamic thylakoid stacking is regulated by LHCII phosphorylation but not its interaction with PSI. Plant Physiol 180: 2152–2166
Google Scholar: Author Only Title Only Author and Title

Yang Y, Benning C (2018) Functions of triacylglycerols during plant development and stress. Curr. Opin. Biotechnol 49: 191– 198
Google Scholar: Author Only Title Only Author and Title

Yoshimoto K, Hanaoka H, Sato S, Kato T, Tabata S, Noda T, Ohsumi Y (2004) Processing of ATG8s, ubiquitin-like proteins, and their deconjugation by ATG4s are essential for plant autophagy. Plant Cell.16: 2967–2983.
Google Scholar: Author Only Title Only Author and Title

Yoshimoto K, Jikumaru Y, Kamiya Y, Kusano M, Consonni C, Panstruga R, Ohsumi Y, Shirasu K (2009) Autophagy negatively regulates cell death by controlling NPR1-dependent salicylic acid signaling during senescence and the innate immune response in Arabidopsis. Plant Cell 21: 2914–2927

Google Scholar: Author Only Title Only Author and Title

Ytterberg AJ, Peltier JB, van Wijk, KJ (2006). Protein profiling of plastoglobules in chloroplasts and chromoplasts. A surprising site for differential accumulation of metabolic enzymes. Plant Physiol. 140: 984–997.

Google Scholar: Author Only Title Only Author and Title

Zhao L, Dai J, Wu Q (2014) Autophagy-like processes are involved in lipid droplet degradation in Auxenochlorella protothecoides during the heterotrophy–autotrophy transition. Front Plant Sci 5: 400.

Google Scholar: Author Only Title Only Author and Title